Arabidopsis inositol polyphosphate kinases regulate COP9 signalosome functions in phosphate-homeostasis

Yashika Walia[1], Kishor D Ingole[1,2], Mritunjay Kasera[1], Swaroop Peddiraju[1], Gabriel Schaaf[3], and Saikat Bhattacharjee[1*]

[1]Laboratory of Signal Transduction and Plant Resistance, UNESCO-Regional Centre for Biotechnology (RCB), NCR Biotech Science Cluster, 3rd Milestone, Faridabad-Gurgaon Expressway, Faridabad- 121 001, Haryana, India.

[2]Kalinga Institute of Industrial Technology (KIIT) University, Bhubaneswar- 751 024, Odisha, India.

[3]Department of Plant Nutrition, Institute of Crop Science and Resource Conservation, Rheinische Friedrich-Wilhelms-Universität Bonn, 53115 Bonn, Germany.

*Corresponding author:

Saikat Bhattacharjee

saikat@rcb.res.in

Tel: (+91) 0129-2848837

ORCID ID

Saikat Bhattacharjee https://orcid.org/0000-0003-1369-7700

Gabriel Schaaf https://orcid.org/0000-0001-9022-4515

Yashika Walia https://orcid.org/0000-0001-8122-8661

Kishor D Ingole https://orcid.org/0000-0003-1946-6639

Mritunjay Kasera https://orcid.org/0000-0002-1110-3502

Swaroop Peddiraju https://orcid.org/0000-0001-5290-7067

Abstract

Targeted protein degradation is essential for physiological development and adaptation to stress. Mammalian INOSITOL PENTAKISPHOSPHATE KINASE (IP5K) and INOSITOL HEXAKISPHOSPHATE KINASE 1 (IP6K1) pair modulates functions of Cullin RING Ubiquitin E3 ligases (CRLs) that execute targeted degradation of substrates. Coordinated activities of these kinases protect CRLs on a COP9 signalosome (CSN) platform and stimulates deneddylation-dependent disassembly to maintain continuity of its functions. In plants, CRL regulations on CSN by inositol phosphate (InsP) kinases are not known. Here, we show interactions of *Arabidopsis thaliana* INOSITOL PENTAKISPHOSPHATE 2-KINASE 1 (IPK1) and INOSITOL 1,3,4-TRISPHOSPHATE 5/6-KINASE 1 (ITPK1), counterparts of the above InsP-kinase pair, with CSN subunits and its positive influences on the dynamics of cullin deneddylation. We identify neddylation enhancements on CRLs as an early response to phosphate-starvation and its orchestration by perturbed IPK1/ITPK1 activities. At a molecular level, specific kinetics of CSN5 deneddylase is affected by the above InsP-kinases. Overall, our data reveal conserved InsP-kinase involvements on CRL-CSN synergism in plants.

41 **Introduction:**

42 The versatile functions of inositol phosphates (InsPs) in multiple cellular processes of all
43 eukaryotes is owed to its propensity for differential degree of phosphorylation catalyzed by
44 relatively conserved set of InsP-kinases[1-4]. In plants, $InsP_6$ (myo-inositol-1,2,3,4,5,6-
45 hexakisphosphate or phytic acid), produced by INOSITOL PENTAKISPHSPHATE 2-
46 KINASE 1 (IPK1) is sequentially (pyro)-phosphorylated by INOSITOL 1,3,4-
47 TRISPHOSPHATE 5/6-KINASES (ITPK1/2) and then by DIPHOSPHOINOSITOL
48 PENTAKISPHOSPHATE KINASES (PPIP5K or VIH1/2) to generate energy-rich
49 phosphoanhydride bond-containing inositol pyrophosophates (InsPP) $InsP_7$ and $InsP_8$,
50 respectively[5-8]. While $InsP_6$ or more recently speculated $InsP_7$, promotes auxin-dependent
51 degradation of AUX/IAA repressors, $InsP_8$ targets JASMONATE ZIM-DOMAIN (JAZ)
52 repressors[7,9-11]. Reduced $InsP_8$ levels during phosphate (Pi)-deprivation liberates the
53 transcription factor PHOSPHATE STARVATION RESPONSE 1 (PHR1)[12] to cause activation
54 of phosphate-starvation inducible (PSI) genes, but also subsequently targets its captor SPX1
55 (SYG1/Pho81/XPR1-domain containing protein1) for 26S proteasome-mediated
56 degradation[13-17]. Taken together, roles of InsP(P)s clearly include biochemical regulators of
57 stimulus-dependent substrate stabilities.

58 In a typical eukaryotic cell, ~20% of targeted protein degradation are mediated by Cullin RING
59 E3 ubiquitin ligases (CRLs)[18,19] that require covalent modification of a Nedd8 moiety on cullins
60 (CULs) (a process termed as neddylation)[19]. In absence of cognate substrates self-
61 ubiquitinylation-vulnerable CRLs are protected on Constitutive photomorphogenesis 9
62 signalosome (CSN), an evolutionarily conserved eight-subunit (CSN1-8) macromolecular
63 complex[20,21]. The CSN5 subunit in this complex contains an MPN+/JAMM metalloprotease
64 motif that catalytically removes Nedd8 (deneddylation) from CULs[22] causing CRL
65 disassembly and promoting newer associations required for continuum of its functions.

66 Optimal CRL activity hence necessitates regulated neddylation/deneddylation cycles of CULs.
67 Apparent contradiction between genetic requirements of the CSN-protection versus its
68 deneddylation activity on CRLs forms the basis of the 'CSN paradox'[23]. In mammals, locale-
69 specific coordinated activities of IP5K with IP6K1, functional homologs of Arabidopsis IPK1
70 and ITPK1, respectively provide $InsP_6$ to strengthen or $InsP_7$ to loosen CRL-CSN
71 associations[24-26]. Interaction changes affect cellular ratio of neddylated CUL: unneddylated
72 CUL (CUL^{Nedd8}:CUL)[26]. Here we show that Arabidopsis IPK1-ITPK1 pair retains conserved
73 CSN interactions and modulate CSN5 deneddylase dynamics. Pi-deprivation is perceived early
74 at CSN, and causes a shift in equilibrium of CRL deneddylation cycle via a response that
75 precedes PHR1-mediated transcriptional changes. Inhibitions of IPK1, ITPK1 or CSN5
76 activities result in constitutive phosphate-starvation response (PSR) even under sufficient Pi
77 availability. However, when actually Pi-starved, PSR responses are suppressed in these plants.
78 Our investigations reveal linked activities of IPK1-ITPK1 pair on CRL-CSN regulations of Pi-
79 homeostasis in plants.

80

81 **Results**

82 **Arabidopsis IPK1 and ITPK1 interact with CSN holo-complex.** Mammalian IP5K co-
83 precipitates with CSN2/5 whereas IP6K1 interacts with CSN1/2[25,26]. Arabidopsis ITPK1 has
84 been previously reported to associate with CSN1[27]. Interactions of Arabidopsis IPK1 with CSN
85 subunits have not been investigated earlier. We immuno-enriched Myc-IPK1 or ITPK1-GFP
86 from *ipk1-1*:*Myc-IPK1* and *itpk1-2*:*ITPK1-GFP* transgenic lines, respectively and probed for
87 the presence of selective CSN subunits, CUL1 or the substrate adaptor ASK1. These transgenic
88 lines restore high endogenous Pi and elevated PSI-gene *SPX1* expressions to wild-type (Col-0)
89 levels implicating the functionality of the corresponding fusion proteins[9] (Extended Data Fig.

90 1). In immunoprecipitation assays, CSN1/2/4/5, CUL1 and ASK1 co-purified with IPK1,
91 whereas ITPK1 enrichments detected CUL1, ASK1, and CSN1/2 but not CSN4/5 subunits
92 (Fig. 1a-b). This matches mammalian ITPK1 interactions with CSN1 but not CSN5[28]. Through
93 Biomolecular Fluorescence Complementation (BiFC) assays IPK1 or ITPK1 association with
94 CSN1 and CSN2 are detected as nucleocytoplasmic complexes similar to localization of the
95 individual proteins[6] (Fig. 1c-d; Extended Data Fig. 2). A negative control β-Glucuronidase
96 (GUS) protein does not interact with IPK1, ITPK1 or CSN1/2 (Extended Data Fig. 2). These
97 data suggest that likewise to animals, CSN associations of IPK1 and ITPK1 are conserved in
98 Arabidopsis. Although biochemically coupled through substrate-product relationship,
99 interaction between IPK1 and ITPK1 has not been demonstrated *in planta*. To this end, we
100 performed co-immunoprecipitation assays via transient co-expression of Myc-IPK1 and GFP-
101 ITPK1. Enrichment of GFP-ITPK1 with anti-GFP affinity beads co-elutes Myc-IPK1
102 indicating their associations *in vivo* (Fig. 1e). As earlier, via BiFC IPK1-ITPK1 complexes are
103 detected at nucleocytoplasmic locales (Extended Data Fig. 2). Interaction assays *in vitro* with
104 recombinant His-IPK1 and GST-ITPK1 further confirm direct association between these
105 proteins (Fig. 1f). Overall, our results recapitulate IPK1 and ITPK1 interactions with CSN and
106 with each other.

107 To determine the cellular proportions of IPK1 or ITPK1 that associate with or are independent
108 of the CSN holo-complex, we subjected Col-0, *ipk1-1*:*Myc-IPK1* and *itpk1-2*:*ITPK1-GFP*
109 extracts to size-exclusion chromatography followed by immunoblots for detecting
110 representative CSN subunits, Myc-IPK1 or ITPK1-GFP. The elution patterns of molecular
111 weight standards and selective CSN subunits with demarcation of CSN holo-complex fractions,
112 as noted in several earlier reports are shown[29,30] (Fig. 2a). CSN1, exclusively associates with
113 the CSN holo-complex and elutes accordingly in higher molecular weight pools (400-600 kDa).
114 CSN5 fractionates both as a part of CSN holo-complex as well as in lower molecular weight

115 pools (monomers, 100-50 kDa). Partitioning profiles of CSN5 and CSN4 are comparable
116 between Col-0, *ipk1-1*:*Myc-IPK1* and *itpk1-2*:*ITPK1-GFP* (Fig. 2c; Extended Data 3).
117 Remarkably, neither Myc-IPK1 nor ITPK1-GFP proteins are detected in fractions
118 corresponding to the CSN holo-complex implying that these associations are either transient
119 or represent only a marginal proportion of these proteins (Fig. 2a). Co-elution of Myc-IPK1
120 and ITPK1-GFP in overlapping fractions is likely indicative of their *in vivo* associations we
121 noted earlier.

122 **CSN5 deneddylase deficiencies of CSN cause enhanced CUL1 neddylation in *ipk1* or *itpk1***
123 **mutant.** Depletion of IP5K or IP6K1 reduces CRL-CSN associations in mammalian
124 systems[24,25]. To examine whether in *ipk1-1* or *itpk1-2* lower CUL1 pools co-fractionate with
125 the CSN holo-complex, extracts from these plants and Col-0 were fractionated as earlier and
126 compared for elution profiles of CSN subunits and CUL1. Although CSN1/4 or CUL1 profiles
127 are comparable (Fig. 2a-b; Extended Data 3), increased CSN5 presence in fractions
128 corresponding to CSN holo-complex with a concomitant decrease in the monomeric elutions
129 is apparent for *ipk1-1* or *itpk1-2* when compared to Col-0 (Fig. 2c). Total levels of CSN5
130 however are unaffected in these mutants. Taking into account that overall CUL1 profiles are
131 comparable, CRL assemblies or CRL-CSN associations are likely not perturbed in the *ipk1-1*
132 or *itpk1-2* plants. Immuno-enrichments of CUL1 although is slightly lower from *ipk1-1* or
133 *itpk1-2* than Col-0, nonetheless proportionately similar amounts of CSN1/2 as in Col-0 are
134 bound to it further supporting the above conclusion (Extended Data Fig. 4).

135 Resident CSN5 performs the deneddylase role in a CSN holo-complex[22]. This raised the
136 intriguing possibility whether changed partitioning of CSN5 in *ipk1-1* or *itpk1-2* impact CSN-
137 mediated deneddylation efficiencies on CRLs. Indeed, as a consequence of depleting IP5K or
138 IP6K1 in mammalian system steady-state ratio of $CUL1^{Nedd8}$:CUL1 are perturbed to cause
139 strong increments in CUL^{Nedd8} levels[25,26]. Remarkably, in *ipk1-1* or *itpk1-2* lysates, enhanced

140 CUL1^{Nedd8} levels relative to Col-0 are strikingly prominent (Fig. 2d). Extracts from *ipk2β-1*
141 with low $InsP_6$ levels as *ipk1-1*[2], or *vih2-4* plants with elevated $InsP_7$ [7] does not show elevated
142 CUL1^{Nedd8} pools as in *ipk1-1* or *itpk1-2* (Extended Data Fig. 5). A modest decrease in
143 CUL1^{Nedd8}:CUL1 ratio is however consistently noted in *ipk2β-1*. In the respective
144 complemented lines of *ipk1-1* or *itpk1-2*, CUL^{Nedd8}:CUL ratios are restored comparable to Col-
145 0 (Fig. 2d).

146 Global ubiquitinylation is enhanced due to loss of mammalian IP6K1[25]. As a possible
147 consequence to increased CUL^{Nedd8} levels, we tested relative levels of ubiquitinylation in Col-
148 0, *ipk1-1*, or *itpk1-2* extracts. Clear increase in global ubiquitin-conjugates in appearance of a
149 smear when probed with anti-ubiquitin antibodies is detected in the mutant plants than Col-0
150 (Fig. 2e). In complemented lines, wild-type ubiquitinylation levels are noted. Further, in-lysate
151 deneddylation assay to determine deneddylase defects[24] reveal decreased efficiencies of CUL1-
152 deneddylation by endogenous CSN5 simultaneous with increased CUL1 turnover rates in *ipk1-*
153 *1* or *itpk1-2* extracts (Fig. 2f). This decrease in stability likely accounts for the reduced
154 immuno-enrichments from the mutants observed earlier. Taken together, our results parallel
155 animal studies and point to impaired CSN-deneddylation activity in *ipk1-1* or *itpk1-2*, that lead
156 to augmented CUL1^{Nedd8}:CUL1 ratios with increased CUL1 turnover due to self-
157 ubiquitinylation.

158 **Down-regulation of CSN deneddylase activity resulting in increased CUL1 neddylation**
159 **occur during PSR.** Common consequences in *ipk1-1* and *itpk1-2* are auxin-insensitivity and
160 constitutive expression of PSI-genes[9,31-33]. Reduced $InsP_8$, common to *ipk1-1* or *itpk1-2*, likely
161 disrupt SPX1-PHR1 interactions leading to activation of PSI-genes[34]. MLN4924, a small
162 molecule pharmacological inhibitor of CUL neddylation[18] is functional in Arabidopsis, inhibits
163 degradation of CRL substrates and confers auxin insensitivity[35]. To test whether increased PSI-

164 gene expressions in *ipk1-1* or *itpk1-2* are consequences of enhanced CUL1-neddylation, we
165 treated these plants with MLN4924. Remarkably, elevated expression of PSI-genes such as
166 *PHT1;3, SPX1,* or *IPS1* as well as high endogenous Pi levels in *ipk1-1* or *itpk1-2* are reduced
167 upon MLN4924-treatment (Fig. 3a-b). In Col-0 grown under Pi-sufficient conditions,
168 MLN4924 treatments did not cause detectable change in endogenous Pi-levels or *IPS1*
169 expression (Fig. 3b; Extended Data Fig. 11). Most surprisingly, MLN4924 treatments
170 suppressed the induction of *PHT1;3* or *IPS1* in Col-0 when subjected to Pi-starvation (Fig. 3c).

171 To test whether neddylation efficiencies of cullins are affected upon Pi-deprivation, extracts
172 from Col-0 grown under Pi-replete or exposed to Pi-deplete conditions were immunoblotted
173 with anti-CUL1 antibodies. Prominent increase in $CUL1^{Nedd8}$ levels, sensitive to MLN4924
174 inhibition, was noted in Col-0 when shifted from Pi-replete to Pi-deplete conditions (Fig. 3d).
175 Basally enhanced levels of $CUL1^{Nedd8}$ in *ipk1-1* or *itpk1-2* remain unchanged under Pi-deplete
176 conditions (Extended Data Fig. 6). Surprisingly, enhancements of CUL^{Nedd8} levels under Pi-
177 deplete conditions also occur in the PSR-defective *phr1phl1* plants implicating that neddylation
178 readjustments are upstream of PHR1/PHL1 (PHR1-LIKE 1) role in inducing PSI-gene
179 expressions (Fig. 3d). Our assays hence identify CUL1 hyperneddylation as an early response
180 to Pi-starvation essential to transduce downstream signaling.

181 Interestingly, in-lysate denddylation assay on Pi-starved Col-0 although shows diminished
182 CSN5 deneddylase activity, nevertheless unlike noted for *ipk1-1* or *itpk1-2*, CUL1 instabilities
183 are not accentuated (Extended Data Fig. 7). Also, CSN5 elution profiles under Pi-deplete
184 conditions are peculiarly similar to patterns in *ipk1-1* or *itpk1-2* with more engagements in the
185 CSN holo-complex fractions but no change in its total protein levels (Fig. 3e). Curiously, unlike
186 *ipk1-1* or *itpk1-2*, global ubiquitinylation are not enhanced upon Pi-starvation (Fig. 3f).
187 Together, these results indicate highly coordinated CRL-activities on substrates to maintain
188 specificity in responding to reduced Pi-availability. Combined, our data also suggest that Col-

189 0 plants tone-down CSN-deneddylase activity during Pi-deprivation to induce PSI-gene
190 expressions, a phenomenon that is constitutive in *ipk1-1* or *itpk1-2*. Overall fractionation
191 profiles of CSN1, or CUL1 remain unaltered by the Pi-changes (Extended Data Fig. 8a). We
192 also detect marked and modest increase in ITPK1-GFP and Myc-IPK1 protein levels,
193 respectively in Pi-starved extracts although their transcription efficiencies remain largely
194 unchanged[33] (Extended Data Fig. 8b). This is suggestive of possible modulations of their kinase
195 activities brought about by the increased accumulation and needs to be investigated further.
196 Together, with these observations, it is evident that CSN5 dynamics of the CSN is altered under
197 Pi-starvation.

198 **CSN5 loss or inhibition phenocopies *ipk1* or *itpk1* mutant responses.** To determine whether
199 PSI-gene expressions are globally affected by CSN functions, we mined the available
200 microarray data of differentially expressed transcripts in *csn* null mutants (*csn3*, *csn4* and
201 *csn5ab*)[36]. Strong upregulation in expressions compared to wild-type plants are especially
202 noted in genes responsible for Pi-remobilization (*PAP1, PAP10, PAP23, DFR, F3H*) and a few
203 Pi-transporters (*PHT3;2, PHT3;3, OCT1*), categorized earlier[31] (Extended Data Fig. 9).
204 Expressions of *PHR1* or *PHL1* remain unaffected as in *ipk1-1* or *itpk1-2* [31,32]. Neither *IPK1* nor
205 *ITPK1* transcriptions are changed in the *csn* mutants. Thus, CSN holo-complex defects overall
206 affect several PSI-gene expressions likely because of its deneddylation-deficiencies. To
207 explore CSN roles further, we utilized the *csn5a-2* plants (SALK_027705) harboring a T-DNA
208 insertion in the last exon of the *CSN5A* isoform (*At1g22920*). Similar to *ipk1-1* or *itpk1-2*,
209 *csn5a-2* extracts accumulate higher $CUL1^{Nedd8}$ levels and display auxin-insensitivity [9,29,30,36].
210 Under Pi-replete conditions, mild increase in basal Pi-levels accompanied by up-regulated
211 expressions of *PHT1;3* or *IPS1* is detected in the *csn5a-2* plants (Fig. 4a-b). These parallel
212 phenomena in *ipk1-1* or *itpk1-2*. Upon exposure to Pi-deplete conditions, and in contrast to
213 Col-0, *csn5a-2* plants are completely impaired in inducing *PHT1;3* or *IPS1* (Fig. 4b).

214 Strikingly, these results also resemble deficiencies in *itpk1-2* when subjected to Pi-starvation[33]
215 suggesting that CSN5 processes are linked to maintenance of Pi-homeostasis and successful
216 transduction of PSR.

217 To further substantiate CSN5 involvement, we tested the effects of recently reported CSN5
218 inhibitors Azaindole#6 and CSN5i-3 on Arabidopsis PSR[37,38]. In animal cell lines, these
219 inhibitors interfere with CSN5 deneddylase activity and trap CRLs in their neddylated states.
220 Because they remain untested in any plant systems, we first determined their efficacy on
221 Arabidopsis seedlings. Parallel MLN4924 treatments were used as neddylation-inhibition
222 controls. Dose-dependent increments in $CUL1^{Nedd8}$ levels with collateral decrease in
223 unneddylated-CUL1 are detected at 24hr post-treatment with CSN5i-3 (Fig. 4c). Even at 48-
224 hrs post-treatment, CSN5i-3 inhibitions are maintained (Extended Data Fig. 10). At all doses
225 tested, Azaindole#6 remained ineffective in changing $CUL1^{Nedd8}$: CUL1 ratios. As expected,
226 MLN4924 treatments in a dose-dependent manner reduce $CUL1^{Nedd8}$ levels. For subsequent
227 experiments, we continued with 10μM dose of CSN5i-3 and the same for MLN4924, as used
228 in earlier assays. On Col-0, CSN5i-3 caused a modest increase in basal Pi levels and
229 upregulation in expression of *PHT1;3*, but not significantly for *SPX1* or *IPS1*(Fig. 4d-e;
230 Extended Data Fig. 11a). Under Pi-deplete exposure, CSN5i-3 dramatically suppressed the
231 induction of *PHT1;3, SPX1* or *IPS1* in Col-0 and mirrored MLN4924 effects (Fig. 4e; Extended
232 Data Fi. 11a-b). CSN5i-3-treated Col-0 extracts when fractionated, CSN5 was clearly more
233 enriched in the CSN holo-complex pools resembling *ipk1-1*, *itpk1-2,* or Pi-starved profiles (Fig.
234 4f). With these results, we once again envision strong connection between CSN5 deneddylation
235 deficiencies in *ipk1-1* or *itpk1-2* plants to defects in CSN5 dynamics on CSN. Most
236 interestingly, *ipk1-1* or *itpk1-2* seedlings grown under sufficient Pi when treated with CSN5i-
237 3 have reduced *IPS1* expressions than untreated plants indicating that skewed kinetics of CSN5
238 rather complete deficiency in its functions is attributed to these mutants (Extended Data Fig.

239 11b). MLN4924-treatments on *ipk1-1* or *itpk1-2* in Pi-deplete growth medium offer relief by
240 elevating *IPS1* expressions further supporting our hypothesis that inadequacies in these
241 mutants to support PSR is related to dynamics of CSN5-regulated neddylation/deneddylation
242 cycles (Extended Data Fig. 11). From these results, it is imperative that IPK1/ITPK1 functions
243 influence CSN5 dynamics thus affecting the deneddylase activity of CSN holo-complex and
244 its role in executing PSR.

245 **ITPK1 activity primarily regulates CSN5 deneddylase functions of CSN.** $InsP_6$ rather than
246 $InsP_7$ is implicated as the physiological glue in potentiating CSN2-CRL associations[26]. That a
247 kinase-dead IP5K interacts weakly with CSN2/5 further implies that $InsP_6$ augmenting these
248 interactions is produced locally. Supplementing $InsP_6$ to IP5K-depleted cell lysates strengthens
249 CRL-CSN2 associations, and increases deneddylation rates of recombinant CSN on purified
250 neddylated cullins[26]. Apparently, the externally added metabolite gains access to its designated
251 binding pocket at the CRL-CSN2 interface. Even though CRL-CSN associations are not
252 affected in *ipk1-1* or *itpk1-2*, we investigated whether adding $InsP_6$ to lysates recover
253 deneddylation deficiencies in the mutants, or cause its augmentation in Col-0. Our results
254 clearly show that externally added $InsP_6$ does not alter deneddylation defects or CUL1
255 instability in *ipk1-1* or *itpk1-2* (Extended Data Fig. 12a). In Col-0 extracts, $InsP_6$
256 supplementation does not change deneddylation rates or stability of CUL1 indicating that
257 unlike mammalian systems, CSN functions in plants are not influenced by $InsP_6$.

258 Unlike $InsP_6$, the CRL-CSN release factor $InsP_7$ when supplemented to mammalian cell
259 extracts does not lead to complex disassembly[25]. This means that IP6K1 activity is very tightly
260 regulated spatiotemporally. With observed ITPK1-CSN2 interactions, this instigated us to
261 investigate whether CSN5 deneddylation deficiency in *ipk1-1* or *itpk1-2* is directly associated
262 with impaired ITPK1 activity. The cell-permeable compound TNP inhibits animal IP6K1
263 functions and reduce $InsP_7$ levels[39]. In 10μM TNP-treated Col-0 extracts, distinct increase in

264 CUL1^{NEDD8} levels are observed although less potent to a similar dose of CSN5i-3 (Fig. 5a). We
265 used 25μM TNP doses for subsequent assays. In Col-0 grown in Pi-sufficient media, TNP
266 presence replicated CSN5i-3 results in augmenting basal Pi levels, upregulation of *IPS1* or
267 *SPX1* expressions, and more retention of CSN5 in the CSN holo-complex pools (Fig. 5b; Fig.
268 4f). TNP also suppressed endogenous deneddylation rates with increased CUL1 instability
269 (Fig. 5c). And likewise to CSN5i-3, TNP also suppressed PSI-gene inductions in Col-0 under
270 Pi-deplete circumstances (Fig. 5b). With these results, we provide convincing evidence of
271 ITPK1 activity-regulated CSN(5) implications in maintenance of Pi-homeostasis and PSR.
272 Overall, with our data we present localized coordinated activities of IPK1-ITPK1 pair in
273 modulating CSN dynamics, defining molecular concept of the CSN paradox, and underlining
274 CSN role in phosphate stress responses of plants.

275

276 **Discussion**

277 In animal systems, CRL-CSN tether is augmented by $InsP_6$ and released via stimulus-driven
278 $InsP_7$ synthesis. Here, we show that although Arabidopsis IPK1 and ITPK1 retain conserved
279 CSN interactions, $InsP_6$/$InsP_7$ changes in the corresponding mutants do not overall affect
280 CRL1-CSN associations. Thus, either the residual levels of these InsPs suffice at the CRL-CSN
281 junctures or the association/dissociation cycles involve an altogether different InsP(s) not
282 locally altered in the above mutants. That, unlike mammalian results, added $InsP_6$ does not
283 rescue *ipk1-1* or even alter CUL1 deneddylation rates/stability in Col-0 is supportive of strict
284 coordinated roles of IPK1-ITPK1 pair at CSN locales. Data showing an *ITPK4* mutant (*itpk4-*
285 *1*) with reduced $InsP_6$/$InsP_7$ as *ipk1-1* or *itpk1-2* has normal PSR[32] and Col-0 comparable ratio
286 of CUL1^{Nedd8}:CUL1 (Extended Data Fig. 12b) also lends support to our hypothesis. However,
287 in one striking distinction both *ipk1-1* or *itpk1-2* accumulate increased levels of Ins(3,4,5,6)P_4

288 which neither the *itpk4-1* nor Col-0 subjected to PSR does[32]. Whether the recently reported
289 reversibility of Ins(3,4,5,6)P_4 to InsP_7 synthesis catalyzed by substrate-product related IPK1-
290 ITPK1 pair and strongly influenced by cellular energy status in principle affects CSN functions
291 need to be investigated further[33,40,41]. In all regards, our model (Fig.5e) proposing that
292 decreased CSN5 deneddylase performance and lower CUL1 deneddylation rates due to loss of
293 IPK1 or ITPK1 nevertheless implicates their activities in CSN roles on CRLs. With previously
294 known effects of mammalian ITPK1 over-expression on CSN5 equilibrium [28], we show here
295 the similar phenomenon in absence/upon inhibition of either ITPK1 or CSN5 revealing
296 intricately choreographed plant ITPK1 role on CSN5 dynamics especially its entry-exit shuttles
297 and deneddylase activity.

298 With obvious InsP_8 reduction in *ipk1-1*, *itpk1-2* or upon Pi-starvation, PHR1 liberated from
299 SPX1 causes activation of PSI-gene expressions. In turn, SPXs undergo ubiquitination by
300 homologs of recently identified rice ubiquitin E3 ligases SDEL1/2[13,14,17,42]. Here we
301 demonstrate that perception of Pi-deprivation is accompanied by PHR1/PHL1-independent
302 increase in CUL1 neddylation, a feature mimicked constitutively by ITPK1 loss/inhibition and
303 suppressed by the neddylation inhibitor MLN4924. Pronounced CSN5 retentions on CSN holo-
304 complex along with dampened deneddylation rates facilitate more available pools of
305 neddylated CRLs to ubiquitinylate SPX1 and other substrates. This is evident from
306 constitutively enhanced global pool of ubiquitinylated proteins in *ipk1-1* or *itpk1-2* extracts. In
307 Pi-starved plants, this ubiquitinylation is tightly regulated and restricted to intended substrates,
308 such as SPX1, without notably changing global polyubiquitin-conjugates. Failure to respond
309 under low-Pi and induce PSI-gene upregulations in *itpk1-2*[33] or by inhibition of ITPK1 or
310 CSN5, indicates that the observed CSN5 partitioning changes upon Pi-starvation is only a
311 transitory shift of deneddylase kinetics, and not complete inhibition of its activity. And CRLs
312 continue to require neddylation/deneddylation cycles to successfully transduce PSR. This again

313 may be linked to InsPs generated by reverse reactions of IPK1-ITPK1 pair under changed
314 adenylate charge as occurring during Pi-starvation[33,40]. Overall, with our data we highlight
315 IPK1-ITPK1 role in CSN regulations that addresses key aspects of its multi-faceted functions
316 in responding to Pi-imbalances.

317

318 **References**

319 1 Raboy, V. Accumulation and Storage of Phosphate and Minerals. *Cellular and*
320 *Molecular Biology of plant Seed Development*, 441-477, doi:10.1007/978-94-015-
321 8903-3_12 (1997).
322 2 Stevenson-Paulik, J., Bastidas, R. J., Chiou, S. T., Frye, R. A. & York, J. D. Generation
323 of phytate-free seeds in Arabidopsis through disruption of inositol polyphosphate
324 kinases. *Proc Natl Acad Sci U S A* **102**, 12612-12617, doi:10.1073/pnas.0504172102
325 (2005).
326 3 Monserrate, J. P. & York, J. D. Inositol phosphate synthesis and the nuclear processes
327 they affect. *Curr Opin Cell Biol* **22**, 365-373, doi:10.1016/j.ceb.2010.03.006 (2010).
328 4 Shears, S. B. & Wang, H. Inositol phosphate kinases: Expanding the biological
329 significance of the universal core of the protein kinase fold. *Adv Biol Regul* **71**, 118-
330 127, doi:10.1016/j.jbior.2018.10.006 (2019).
331 5 Desai, M. *et al.* Two inositol hexakisphosphate kinases drive inositol pyrophosphate
332 synthesis in plants. *Plant J* **80**, 642-653, doi:10.1111/tpj.12669 (2014).
333 6 Adepoju, O. *et al.*, doi:10.1101/724914 (2019).
334 7 Laha, D. *et al.* VIH2 Regulates the Synthesis of Inositol Pyrophosphate InsP8 and
335 Jasmonate-Dependent Defenses in Arabidopsis. *Plant Cell* **27**, 1082-1097,
336 doi:10.1105/tpc.114.135160 (2015).

337 8 Laha, D. *et al.* Arabidopsis ITPK1 and ITPK2 Have an Evolutionarily Conserved Phytic
338 Acid Kinase Activity. *ACS Chem Biol* **14**, 2127-2133,
339 doi:10.1021/acschembio.9b00423 (2019).
340 9 Laha, N. P. *et al.*, ITPK1-Dependent Inositol Polyphosphates Regulate Auxin
341 Responses in *Arabidopsis thaliana*. *BioRxiv preprint* doi:10.1101/2020.04.23.058487
342 (2020).
343 10 Sheard, L. B. *et al.* Jasmonate perception by inositol-phosphate-potentiated COI1-JAZ
344 co-receptor. *Nature* **468**, 400-405, doi:10.1038/nature09430 (2010).
345 11 Tan, X. *et al.* Mechanism of auxin perception by the TIR1 ubiquitin ligase. *Nature* **446**,
346 640-645, doi:10.1038/nature05731 (2007).
347 12 Bustos, R. *et al.* A central regulatory system largely controls transcriptional activation
348 and repression responses to phosphate starvation in Arabidopsis. *PLoS Genet* **6**,
349 e1001102, doi:10.1371/journal.pgen.1001102 (2010).
350 13 Lv, Q. *et al.* SPX4 Negatively Regulates Phosphate Signaling and Homeostasis through
351 Its Interaction with PHR2 in Rice. *Plant Cell* **26**, 1586-1597,
352 doi:10.1105/tpc.114.123208 (2014).
353 14 Osorio, M. B. *et al.* SPX4 Acts on PHR1-Dependent and -Independent Regulation of
354 Shoot Phosphorus Status in Arabidopsis. *Plant Physiol* **181**, 332-352,
355 doi:10.1104/pp.18.00594 (2019).
356 15 Puga, M. I. *et al.* SPX1 is a phosphate-dependent inhibitor of Phosphate Starvation
357 Response 1 in Arabidopsis. *Proc Natl Acad Sci U S A* **111**, 14947-14952,
358 doi:10.1073/pnas.1404654111 (2014).
359 16 Rubio, V. *et al.* A conserved MYB transcription factor involved in phosphate starvation
360 signaling both in vascular plants and in unicellular algae. *Genes Dev* **15**, 2122-2133,
361 doi:10.1101/gad.204401 (2001).

362 17 Zhong, Y. *et al.* Rice SPX6 negatively regulates the phosphate starvation response
363 through suppression of the transcription factor PHR2. **219**, 135-148,
364 doi:10.1111/nph.15155 (2018).
365 18 Soucy, T. A. *et al.* An inhibitor of NEDD8-activating enzyme as a new approach to
366 treat cancer. *Nature* **458**, 732-736, doi:10.1038/nature07884 (2009).
367 19 Yi Sun, W. W., Jianping Jin. <CRL Book Sun etal 2020.pdf>. *Advances in*
368 *Experimental Medicine and Biology Biology and Therapeutics* **1217**, doi:10.1007/978-
369 981-15-1025-0 (2020).
370 20 Chamovitz, D. A. & Segal, D. JAB1/CSN5 and the COP9 signalosome. A complex
371 situation. **2**, 96-101, doi:10.1093/embo-reports/kve028 (2001).
372 21 Dubiel, D., Rockel, B., Naumann, M. & Dubiel, W. Diversity of COP9 signalosome
373 structures and functional consequences. *FEBS Lett* **589**, 2507-2513,
374 doi:10.1016/j.febslet.2015.06.007 (2015).
375 22 Cope, G. A. *et al.* Role of predicted metalloprotease motif of Jab1/Csn5 in cleavage of
376 Nedd8 from Cul1. *Science* **298**, 608-611, doi:10.1126/science.1075901 (2002).
377 23 Dubiel, W. Resolving the CSN and CAND1 paradoxes. *Mol Cell* **35**, 547-549,
378 doi:10.1016/j.molcel.2009.08.011 (2009).
379 24 Lin, H. *et al.* Basis for metabolite-dependent Cullin-RING ligase deneddylation by the
380 COP9 signalosome. *Proc Natl Acad Sci U S A* **117**, 4117-4124,
381 doi:10.1073/pnas.1911998117 (2020).
382 25 Rao, F. *et al.* Inositol hexakisphosphate kinase-1 mediates assembly/disassembly of the
383 CRL4-signalosome complex to regulate DNA repair and cell death. *Proc Natl Acad Sci*
384 *U S A* **111**, 16005-16010, doi:10.1073/pnas.1417900111 (2014).

385 26 Scherer, P. C. *et al.* Inositol hexakisphosphate (IP6) generated by IP5K mediates cullin-
386 COP9 signalosome interactions and CRL function. *Proc Natl Acad Sci U S A* **113**, 3503-
387 3508, doi:10.1073/pnas.1525580113 (2016).
388 27 Qin, Z. X., Chen, Q. J., Tong, Z. & Wang, X. C. The Arabidopsis inositol 1,3,4-
389 trisphosphate 5/6 kinase, AtItpk-1, is involved in plant photomorphogenesis under red
390 light conditions, possibly via interaction with COP9 signalosome. **43**, 947-954,
391 doi:10.1016/j.plaphy.2005.08.006 (2005).
392 28 Sun, Y., Wilson, M. P. & Majerus, P. W. Inositol 1,3,4-trisphosphate 5/6-kinase
393 associates with the COP9 signalosome by binding to CSN1. *J Biol Chem* **277**, 45759-
394 45764, doi:10.1074/jbc.M208709200 (2002).
395 29 Dohmann, E. M., Kuhnle, C. & Schwechheimer, C. Loss of the CONSTITUTIVE
396 PHOTOMORPHOGENIC9 signalosome subunit 5 is sufficient to cause the cop/det/fus
397 mutant phenotype in Arabidopsis. *Plant Cell* **17**, 1967-1978,
398 doi:10.1105/tpc.105.032870 (2005).
399 30 Gusmaroli, G., Feng, S. & Deng, X. W. The Arabidopsis CSN5A and CSN5B subunits
400 are present in distinct COP9 signalosome complexes, and mutations in their JAMM
401 domains exhibit differential dominant negative effects on development. *Plant Cell* **16**,
402 2984-3001, doi:10.1105/tpc.104.025999 (2004).
403 31 Kuo, H. F. *et al.* Arabidopsis inositol pentakisphosphate 2-kinase, AtIPK1, is required
404 for growth and modulates phosphate homeostasis at the transcriptional level. *Plant J*
405 **80**, 503-515, doi:10.1111/tpj.12650 (2014).
406 32 Kuo, H. F. *et al.* Arabidopsis inositol phosphate kinases IPK1 and ITPK1 constitute a
407 metabolic pathway in maintaining phosphate homeostasis. *Plant J*,
408 doi:10.1111/tpj.13974 (2018).

409 33 Riemer, E. *et al.*, ITPK1 is an InsP6/ADP phosphotransferase that controls systemic
410 phosphate homeostasis in Arabidopsis. *BioRxiv preprint*
411 doi:10.1101/2020.05.18.100297 (2020).
412 34 Ried, M. K. *et al.*, Inositol pyrophosphates promote the interaction of SPX domains
413 with the coiled-coil motif of PHR transcription factors to regulate plant phosphate
414 homeostasis *BioRxiv preprint* doi:10.1101/2019.12.13.875393 (2019).
415 35 Hakenjos, J. P. *et al.* MLN4924 is an efficient inhibitor of NEDD8 conjugation in
416 plants. *Plant Physiol* **156**, 527-536, doi:10.1104/pp.111.176677 (2011).
417 36 Dohmann, E. M., Levesque, M. P., Isono, E., Schmid, M. & Schwechheimer, C. Auxin
418 responses in mutants of the Arabidopsis CONSTITUTIVE PHOTOMORPHOGENIC9
419 signalosome. *Plant Physiol* **147**, 1369-1379, doi:10.1104/pp.108.121061 (2008).
420 37 Altmann, E. *et al.* Azaindoles as Zinc-Binding Small-Molecule Inhibitors of the JAMM
421 Protease CSN5. *Angew Chem Int Ed Engl* **56**, 1294-1297, doi:10.1002/anie.201608672
422 (2017).
423 38 Schlierf, A. *et al.* Targeted inhibition of the COP9 signalosome for treatment of cancer.
424 *Nat Commun* **7**, 13166, doi:10.1038/ncomms13166 (2016).
425 39 Padmanabhan, U., Dollins, D. E., Fridy, P. C., York, J. D. & Downes, C. P.
426 Characterization of a selective inhibitor of inositol hexakisphosphate kinases: use in
427 defining biological roles and metabolic relationships of inositol pyrophosphates. *J Biol*
428 *Chem* **284**, 10571-10582, doi:10.1074/jbc.M900752200 (2009).
429 40 Whitfield, H. *et al.* An ATP-responsive metabolic cassette comprised of inositol
430 tris/tetrakisphosphate kinase 1 (ITPK1) and inositol pentakisphosphate 2-kinase (IPK1)
431 buffers diphosphosphoinositol phosphate levels. *Biochem J* **477**, 2621-2638,
432 doi:10.1042/BCJ20200423 (2020).

433 41 Wundenberg, T. & Mayr, G. W. Synthesis and biological actions of diphosphoinositol
434 phosphates (inositol pyrophosphates), regulators of cell homeostasis. *Biol Chem* **393**,
435 979-998, doi:10.1515/hsz-2012-0133 (2012).
436 42 Ruan, W. *et al.* Two RING-Finger Ubiquitin E3 Ligases Regulate the Degradation of
437 SPX4, An Internal Phosphate Sensor, for Phosphate Homeostasis and Signaling in Rice.
438 *Mol Plant* **12**, 1060-1074, doi:10.1016/j.molp.2019.04.003 (2019).
439 43 Enchev, R. I. *et al.* Structural basis for a reciprocal regulation between SCF and CSN.
440 *Cell Rep* **2**, 616-627, doi:10.1016/j.celrep.2012.08.019 (2012).
441 44 Mosadeghi, R. *et al.* Structural and kinetic analysis of the COP9-Signalosome
442 activation and the cullin-RING ubiquitin ligase deneddylation cycle. *Elife* **5**,
443 doi:10.7554/eLife.12102 (2016).
444 45 Jia, X., Chanda, B., Zhao, M., Brunner, A. M. & Beers, E. P. Instability of the
445 Arabidopsis mutant csn5a-2 caused by epigenetic modification of intronic T-DNA.
446 **238**, 53-63, doi:10.1016/j.plantsci.2015.05.015 (2015).
447 46 Bhattacharjee, S., Halane, M. K., Kim, S. H. & Gassmann, W. Pathogen effectors target
448 Arabidopsis EDS1 and alter its interactions with immune regulators. *Science* **334**, 1405-
449 1408, doi:10.1126/science.1211592 (2011).
450 47 Chakrabarty, R. *et al.* PSITE vectors for stable integration or transient expression of
451 autofluorescent protein fusions in plants: probing Nicotiana benthamiana-virus
452 interactions. *Mol Plant Microbe Interact* **20**, 740-750, doi:10.1094/MPMI-20-7-0740
453 (2007).
454 48 Huang, H., Quint, M. & Gray, W. M. The eta7/csn3-3 auxin response mutant of
455 Arabidopsis defines a novel function for the CSN3 subunit of the COP9 signalosome.
456 *PLoS One* **8**, e66578, doi:10.1371/journal.pone.0066578 (2013).

457 49 Kim, S. H. *et al.* The Arabidopsis resistance-like gene SNC1 is activated by mutations
458 in SRFR1 and contributes to resistance to the bacterial effector AvrRps4. *PLoS Pathog*
459 **6**, e1001172, doi:10.1371/journal.ppat.1001172 (2010).
460 50 Chiou, T. J. *et al.* Regulation of phosphate homeostasis by MicroRNA in Arabidopsis.
461 *Plant Cell* **18**, 412-421, doi:10.1105/tpc.105.038943 (2006).

462

463 **Figure legends**

464 **Fig. 1. IPK1 and ITPK1 interact with each other and with selective CSN or CRLs**
465 **components *in planta*. a-b,** Immuno-enrichments of IPK1 **(a)** or ITPK1 **(b)** from
466 corresponding complemented lines (*ipk1-1: Myc-IPK1* or *itpk1-2:ITPK1-GFP*, respectively)
467 and probed with anti-CSN1/2/4/5, anti-CUL1, or anti-ASK1 antibodies. IgG-agarose
468 enrichments were used as negative controls. **c-d,** Bimolecular Fluorescence Complementation
469 (BiFC) assays showing reciprocal combinations of **(c)** IPK1 and **(d)** ITPK1 interact with CSN1.
470 Scale bar=50 μm. **e,** Co-immunoprecipitation of transiently expressed GFP-ITPK1 with Myc-
471 IPK1. Immuno-enrichment was performed with anti-GFP antibody-conjugated agarose and
472 probed with anti-GFP or anti-Myc antibodies. **f,** *In vitro* interactions of IPK1 with ITPK1. His_6-
473 IPK1 was co-expressed with GST alone or GST-ITPK1 in *E. coli* cells. Ni^{2+}NTA-affinity
474 enrichments were probed for His_6-IPK1 or GST-ITPK1 with anti-His or anti-GST antibodies,
475 respectively. Migration positions of molecular weight markers (in kDa) and of His_6-IPK1, GST
476 or GST-ITPK1 are shown on the right or left of each panel, respectively.

477 **Fig. 2. CSN5 partitioning and deneddylase functions are affected in *ipk1-1* or *itpk1-2*. a,**
478 IPK1 or ITPK1 does not co-elute with the CSN holo-complex. **b,** CRL1 fractionation profiles
479 are unchanged between Col-0, *ipk1-1* and *itpk1-2*. **c,** Enhanced CSN5 engagement on CSN
480 holo-complex fractions in *ipk1-1* and *itpk1-2*. For fractionations, extracts were separated by

481 size-exclusion chromatography and immuno-blotted with indicated antibodies. Right panels
482 are immunoblots on input extracts. Fraction numbers are indicated above each lane. Numbers
483 above arrowheads denote elution positions of molecular weight standards (in kDa). **d,**
484 Increased neddylated CUL1 in *ipk1-1* or *itpk1-2*. **e,** Global polyubiquitin-conjugates are
485 enhanced in *ipk1-1* or *itpk1-2*. For **d-e**, Total protein extracts were probed with anti-CUL1,
486 anti-actin, or anti-Ubiquitin antibodies as indicated. **f,** CSN5-deneddylation deficiencies and
487 lower CUL1 half-life in *ipk1-1* or *itpk1-2*. For in-lysate deneddylation assay total protein
488 extracts incubated for indicated times (minutes post-incubation; mpi) were probed with anti-
489 CUL1 antibodies. Migration position of molecular weight standards (in kDa) and neddylated
490 ($CUL1^{Nedd8}$) or unneddylated (CUL1) cullin1 are shown. Anti-actin or Ponceau S staining
491 demonstrate loadings controls.

492 **Fig. 3. CUL1 deneddylation rates are reduced during Pi-starvation.** MLN4924 suppresses
493 **a,** elevated PSI-gene expressions, and **b,** reduces endogenous Pi-levels in *ipk1-1* or *itpk1-2*. **c,**
494 MLN4924 suppresses the induction of *PHT1;3* or *IPS1* expressions in Col-0 upon Pi-
495 starvation. **d,** Enhanced CUL1-neddylation during Pi-deprivation is PHR1/PHL1-independent.
496 **e,** Increased CSN5 partitioning on CSN holo-complex occur upon Pi-starvation. **f,** Global levels
497 of polyubiquitin-conjugates are unperturbed during PSR. Gene expression changes were
498 relative to *MON1* transcripts and reported as fold-change relative to Col-0 levels. Data is
499 presented as mean $\pm$ SD (n=3 biological replicates of 3 plants in each). For Pi-estimation
500 assays, data shown as mean $\pm$ SD (n= 6-7 plants). Asterisks denote significant differences from
501 the reference sample. (Student's *t*-test; $*P<0.05$, $**P < 0.01$; $***P < 0.001$, $***P<0.0001$. ns
502 is not significant). For immunoblots, total protein extracts or fractions were probed with anti-
503 CUL1 or anti-CSN5 or anti-ubiquitin antibodies, as indicated. Ponceau S staining show
504 loadings controls. For Pi-deprivation/MLN4924 treatment assays, Seedlings grown in Pi-
505 replete (625μM Pi) medium were either maintained or transferred to Pi-deplete (10 μM Pi)

506 medium for three additional days in the presence of MLN4294 or absence (DMSO) during the
507 shift, before being analyzed. Positions of molecular weight markers (in kDa) are shown.

508 **Fig. 4. The dynamics of CSN5 is essential for responding to phosphate-starvation. a,**
509 *csn5a-2* plants have elevated endogenous Pi levels. **b,** *csn5a-2* plants are deficient in inducing
510 PSI-genes during Pi-starvation. **c,** CSN5i-3 shows dose-dependent inhibition in CUL1
511 deneddylation. Total protein extracts from Col-0, 24hrs post-treated with indicated doses of the
512 inhibitors mentioned, were probed with anti-CUL1 antibodies. Ponceau S staining shows
513 loading controls. **d,** CSN5i-3 treatment elevates endogenous Pi-levels. **e,** CSN5i-3 suppresses
514 *PHT1;3* induction in Col-0 during phosphate-starvation. **f,** CSN5 is enriched in CSN holo-
515 complex pools upon CSN5i-3 or TNP treatment. Fractionation was performed 24hrs post-
516 inhibitor treatment and fractions immunoblotted with anti-CSN5 antibodies. For Pi-estimation
517 assays, error bars show SD from mean (n=3 replicates of 5-6 plants each). For gene expression
518 changes, *MON1* levels were used as internal controls and results reported as fold-change
519 relative to untreated Pi-replete grown Col-0. Data is mean $\pm$ SD (n=3 replicates, 3-4 plants
520 each). Statistical significance was calculated with Student's *t*-test and depicted with $*P<0.05$,
521 $**P < 0.01$; $***P < 0.001$, $***P<0.0001$. ns is not significant. For Pi-deprivation assays, plants
522 grown in Pi-replete (625µM Pi) media were transferred for 3 days to Pi-deplete (10 µM Pi)
523 media with or without indicated inhibitors before analysis.

524 **Fig. 5. ITPK1 activity regulates CSN5 dynamics and deneddylase functions. a,** TNP
525 treatment enhances pools of neddylated CUL1. Total protein extracts from Col-0 at 24hrs post-
526 inhibitor treatment were immunoblotted with anti-CUL1 antibodies. **b,** TNP treatments
527 increase endogenous Pi-content in Col-0. Error bars are mean $\pm$ SD (n=3 replicates of 5-6 plants
528 each). **c,** TNP suppresses *IPS1* or *SPX1* in Col-0 upon Pi-starvation. For Pi-starvation, plants
529 grown in Pi-replete medium were transferred for 3 days to Pi-deplete medium with or without
530 TNP. Expression levels of *MON1* transcripts was used as internal reference. Error bars denote

531 mean with SD (n=3 biological replicates of 3-4 plants each). Student's *t*-test was used to
532 calculate statistical significance and shown as $^{**}P<0.01$, $^{***}P<0.001$, $^{****}P<0.0001$, ns not
533 significant. **d,** TNP reduces CUL1 deneddylation and increases CUL1 instability. In-lysate
534 deneddylation assay on Col-0 extracts post-24hrs TNP-treatment and then probed with anti-
535 CUL1 antibodies. Ponceau S staining indicates loadings control. **e,** Schematic representation
536 of IPK1-ITPK1 role on CRL-CSN association/dissociation equilibrium in plants. CSN holo-
537 complex platform offers protection to CRLs in absence of ubiquitinylation substrates (E2
538 enzyme prevented from binding due to mutual exclusion[43,44]) utilizing coordinated locale-
539 specific activities (bi-directional white arrows) of IPK1 and ITPK1. Stimulus/energy status-
540 dependent modulation in localized IPK1/ITPK1 activities (InsPs nature unknown; red question
541 mark) is coupled to CRL, CSN5 disassembly and CUL1 deneddylation. Auto-inhibited CSN
542 holo-complex is reconstituted by re-incorporating CSN5. Active CRL-SCF complex binds E2
543 ubiquitin enzyme to cause targeted ubiquitinylation (Ub^n) and degradation of substrates (such
544 as SPX1 or Aux/IAA repressors). Inhibitory functions of TNP, CSN5i-3 and MLN4924 are
545 indicated on the respective processes. CSN subunits are presented as numbers; CUL1, Cullin1;
546 RBX, RING H2 protein1; SA, substrate adapter, N8, Nedd8, IPK1, inactive IPK1, ITPK1,
547 inactive ITPK1, IPK1 InsP, active IPK1, ITPK1 InsP, active ITPK1.

548

549 **Methods**

550 **Plant material and growth conditions.** Seeds of T-DNA insertion lines of *Arabidopsis*
551 *thaliana* (ecotype Col-0) were obtained from the Arabidopsis Biological Resource Center
552 (ABRC). Homozygous *ipk1-1* (SALK_065337[31]), *itpk1-2* (SAIL_65_D03[32]) *ipk2β-1*
553 (SALK_104995[2]) and *csn5a-2* (SALK_027705[45]) were genotyped using T-DNA and
554 respective gene-specific primers listed in Supplementary Table 1. The *vih2-4, itpk1-2:ITPK1-*

555 *GFP,* and *phr1 phl1* plants have been reported earlier[9,31,32]. Seeds were stratified for 2-days at
556 4°C in dark and then sterilized using 30% bleach solution. They were germinated either directly
557 on soil or on ½ strength Murashige and Skoog (MS) Pi-replete (625 μM KH_2PO_4) agar plates
558 in growth chambers maintained at 22°C with 70% Relative humidity (RH) and 16hrs: 8hrs;
559 light: dark having light intensity 100 μmol $\mu m^{-2}s^{-1}$. For fractionation, Pi-starvation assays, and
560 inhibitor treatments, plants grown on media plates as above were transferred 7-days post-
561 germination to liquid ½ MS medium in 12-well sterile culture plates are proceeded accordingly
562 as indicated in respective experiments. For immuno-precipitation assays 4-week-old soil-
563 grown plants were used.

564 **Generation of constructs.** Arabidopsis *IPK1*, *ITPK1*, *CSN1* and *CSN2* cDNAs were amplified
565 via RT-PCR (iScript cDNA Synthesis Kit, Bio-Rad, USA) from total RNA isolated using
566 RNAiso (Takara-Bio, Japan) from 2-week-old Col-0 plants. Primers for these are listed in
567 Supplementary Table 1. Gateway cloning was first performed into *p*DONR 207 and then into
568 *p*BA-Myc[46] (for Myc-IPK1), *p*SITE-2CA[47] (for GFP-ITPK1), nVenus- or cCFP binary
569 vectors[46] (for all the above) using BP and LR Clonase, respectively (Invitrogen, USA). BiFC
570 vectors for GUS expression have been described earlier[46]. The clones were confirmed by
571 sequencing and electroporated into the agrobacterium strain GV3101 for further assays. For
572 generating clones for recombinant protein expression and *in vitro* interaction assays, IPK1 was
573 sub-cloned into *p*ET28a as *BamH*I-*Sal*I fragment while ITPK1 was cloned as into *p*GEX4T-3
574 as *BamH*I-*Xho*I fragment (primers listed in Supplementary Table 1) to generate His_6-IPK1 and
575 GST-ITPK1, respectively.

576 **Bimolecular Fluorescence Complementation (BiFC) assays.** Agrobacterium strains
577 containing the indicated combination of binary vectors were co-infiltrated at equal cell
578 densities into mature *Nicotiana benthamiana* leaves. After 48hrs post-infiltration, tissue

579 sections from the infiltrated patches were viewed under a SP8 confocal microscope (Leica-
580 microsystems, Germany). Images were acquired with both bright field and YFP filters.

581 ***In vitro* interaction assays in *E. coli*.** Bacterial strain BL21-AI (Arabinose inducible;
582 Thermofisher, USA) harboring GST-ITPK1 or GST with His_6-IPK1 plasmids was grown to
583 0.4 OD_{600nm}, induced with 0.1M IPTG and 0.2% L-arabidose overnight at 28°C. Cell pellets
584 were processed according to manufacturer's instructions, bound to Ni^{2+}-NTA beads (Qiagen,
585 Germany) for 3hrs at 4°C with tumbling, washed and eluted with imidazole. Imidazole was
586 removed via dialysis and elute was immuno-blotted with anti-His or anti-GST antibodies.

587 **Generation of transgenic lines.** For generating complemented *ipk1-1:Myc-IPK1*
588 complemented line, *ipk1-1* plants were floral-dipped with the agrobacterium strain containing
589 Myc-IPK1 binary vector. Transgenic plants were selected on phosphinothricin (10μg/ml)
590 containing ½ MS agar plates and propagated to homozygosity and then used for indicated
591 assays.

592 **Pull down assay/Immunoprecipitation assays.** For co-immunoprecipitation assays between
593 Myc-IPK1 and GFP-ITPK1, agro-infiltrated *N. benthamiana* leaves harvested at 48hrs post-
594 infiltration were used. For pull-downs, including from Arabidopsis transgenic lines *ipk1-*
595 *1:Myc-IPK1*, and *itpk1-2:ITPK1-GFP*, extracts were homogenized in cold RIPA buffer [5mM
596 Tris-HCl pH 7.5, 150mM NaCl, 10mM $MgCl_2$, 1mM EDTA, 1% NP-40, 1mM Sodium
597 deoxycholate and 1X protease inhibitor cocktail (Sigma-Aldrich, USA)]. After removing cell
598 debris via centrifugation, the supernatant was pre-cleared with IgG agarose beads (Sigma-
599 Aldrich, USA) at 4°C for 1hr with rotation. The mix was then centrifuged, IgG agarose bead-
600 pellet washed and saved as non-specific controls. The supernatant was added to indicated
601 antibody-conjugated beads (anti-GFP Agarose, BioBharati Life Sciences, India; anti-Myc
602 Agarose, Sigma-Aldrich, USA). After tumbling overnight at 4°C, the mix was centrifuged, and

603 agarose-bead pellet washed 3-times with RIPA buffer. Beads were then resuspended in 1X
604 Laemmli loading dye and used for immunoblots. For CUL1 pull-down, anti-CUL1 antibodies
605 were first bound to Protein A/G agarose (Sigma-Aldrich, USA), washed and then incubated
606 with Arabidopsis extracts prepared in RIPA buffer as above. Binding was allowed overnight at
607 $4^{o}C$ with rotation, washed next day as earlier and processed for immunoblots.

608 **Size-exclusion chromatography of plant extracts.** Gel-filtration protocol was according to
609 Huang et al (2013)[48]. Briefly, 14-day-old plants ground to a fine powder with liquid nitrogen
610 were homogenized in Gel filtration buffer (50mM Tris-HCl pH 7.5, 150mM NaCl, 1mM
611 EDTA, 10% Glycerol, 10mM $MgCl_2$, 1mM DTT, 1mM PMSF and 1X Protease inhibitor
612 cocktail). Homogenates were centrifuged for 10 mins at $4^{o}C$ and supernatant passed through
613 0.2 μM syringe filters. Total protein extracts were fractionated through Superdex 10/300 GL
614 Column (GE- Healthcare, USA) and eluted in the fractionation buffer at 0.2mL/min flow rate.
615 The eluants were TCA (Trichloroacetic acid) precipitated, washed with acetone and
616 resuspended in 1X Laemmli loading dye and used for indicated immunoblots.

617 **qRT-PCR analysis.** cDNAs prepared as earlier, were used for qRT-PCRs with HOT FIREPol
618 EvaGreen qPCR Mix Plus (ROX) (Solis BioDyne, USA) and primer combinations according
619 to the manufacturer's instructions. Primers used are listed in Supplementary Table 1. Reaction
620 was performed on QuantStudio 6 Flex Real-Time PCR system (Applied Biosystems, USA)
621 with three biological and technical replicates. *MON1* (*At2g28390*) expressions were used as
622 internal control[49]. Relative expression was calculated according to the PCR efficiency^-ΔΔCt
623 formula.

624 **Protein extraction and immunoblots.** Total protein extracts from plants were prepared in 6M
625 Urea and used for western blots. For immunodetection, anti-GFP, anti-Myc (BioBharati Life
626 Sciences, India), anti-CSN1, anti-CSN2, anti-CSN4, anti-CSN5, anti-ASK1, anti-CUL1

627 antibodies (ENZO Life Sciences, USA), anti-Actin (Abiocode, USA) were used. The blots
628 were developed using ECL kit (Bio-Rad, USA) and developed in Alpha Image Quant system
629 (GE-Healthcare, USA).

630 **In-lysate deneddylation assay.** In-lysate deneddylayion assay was according to Lin et al
631 (2020)[24]. Briefly, 14-day-old seedlings were quickly homogenized in deneddylayion buffer
632 (10mM Tris-HCl pH7.5, 150mM NaCl and 0.5% NP-40) in absence of protease inhibitors. The
633 extracts were incubated at 37°C for indicated times, reaction stopped by adding Laemmli
634 loading dye to 1X, and then used for immunoblots.

635 **Pi-estimation assay.** Total Pi measurements is according to Chiou et al (2006)[50]. In brief, fresh
636 tissue was frozen with liquid nitrogen and homogenized in extraction buffer (10mM Tris-HCl,
637 1mM EDTA, 100mM NaCl, 1mM PMSF). The homogenized sample was mixed in a ratio of
638 1:9 with 1% glacial acetic acid and incubated at 42°C for 30mins. Then the reaction was mixed
639 in a ratio of 3:7 with Pi-assay solution (0.35% NH_4MoO_4, 0.86N H_2SO_4 and 1.4% ascorbic
640 acid) and incubated at 42°C for 30mins. Pi content was measured at A280 using a
641 spectrophotometer. Standard graph was made with known amounts of KH_2PO_4.

642 **Phosphate-starvation assays.** After germination of seeds as described earlier, seedlings were
643 transferred to liquid ½ MS medium in 12-well sterile culture plates with Pi-replete conditions
644 (625 μM KH_2PO_4) and placed in the growth chamber. After 4-days, the plants were either
645 maintained with Pi-replete or transferred to Pi-deplete (10 μM KH_2PO_4) liquid media and
646 continued for another 3 days (total 14-days post-germination) before being used for Pi-
647 estimation, qRT-PCR, total protein extraction, fractionation assays.

648 **Inhibitor treatments.** Stock solutions of MLN4924 (Cayman Chemicals, USA), CSN5i-3
649 (Novartis Inc, Switzerland), or TNP (Sigma-Aldrich, USA) was prepared in DMSO. For
650 treatments, 10μM final concentration of MLN4924 or CSN5i-3 were used. TNP was used at

651 25μM final unless otherwise indicated. For assays on Col-0, *ipk1-1*, or *itpk1-2* or for
652 fractionations, inhibitors were treated for 24hrs. For effects on PSR, inhibitors were added
653 during the shift to Pi-deplete medium.

654 **Ubiquitination assays.** For determining global ubiquitination levels, extracts from indicated
655 plants prepared in Gel filtration buffer in the presence of 10μM proteasome inhibitor MG132
656 were incubated on ice for 2hrs. Immunoblotting was then performed with anti-ubiquitin
657 antibodies (P4D1; SantaCruz Biotechnology, USA).

658 **Statistical analysis.** All Data presented here are representative of at least three biological and
659 technical replicates for each. Student's *t*-test were applied for statistical analysis.

660

661 **Acknowledgements**

662 We thank Regional Centre for Biotechnology (RCB), Faridabad, for financial support, lab
663 infrastructure, and central instrumental facilities. S.B. expresses gratitude to Department of
664 Biotechnology (DBT), Govt. of India for the award of Ramalingaswami re-entry fellowship
665 and Grant (No. BT/PR23666/AGIII/103/1039/2018) that supported this research. The *phr1*
666 *phl1* double mutant seeds were a gracious gift from by Prof. Tzyy-Jen Chiou, Academia Sinica,
667 Taipei. A crucial part of our investigations would not be possible without the gracious gift of
668 CSN5i-3 from Dr. Eva Altmann, Novartis Institutes for BioMedical Research, Switzerland.
669 Many thanks to Dr. Divya Chandran (RCB) for help with transcriptomic data analysis of *csn*
670 mutants. Y.W. thanks DBT for providing the Young Investigator award to her for pursuing this
671 research. K.D.I. acknowledges DBT for providing fellowships and KIIT University his PhD
672 registrations. M.K. thanks UGC for his PhD fellowship. All authors thanks Dr. Nripendra Singh

673 and his team at Advanced Technology Platform Centre (ATPC), Faridabad, India for constant
674 support with sample fractionations.

675 **Author Contributions**

676 Y.W. and S.B. conceived and designed the research. Y.W. and S.B. performed most of the
677 experiments. Y.W., K.D.I, M.K., and S.P. conducted and analyzed gene/protein expression
678 changes. Y.W. and S.B. wrote the manuscript.

679 **Competing interests**

680 The authors declare no conflict of interest for this study.

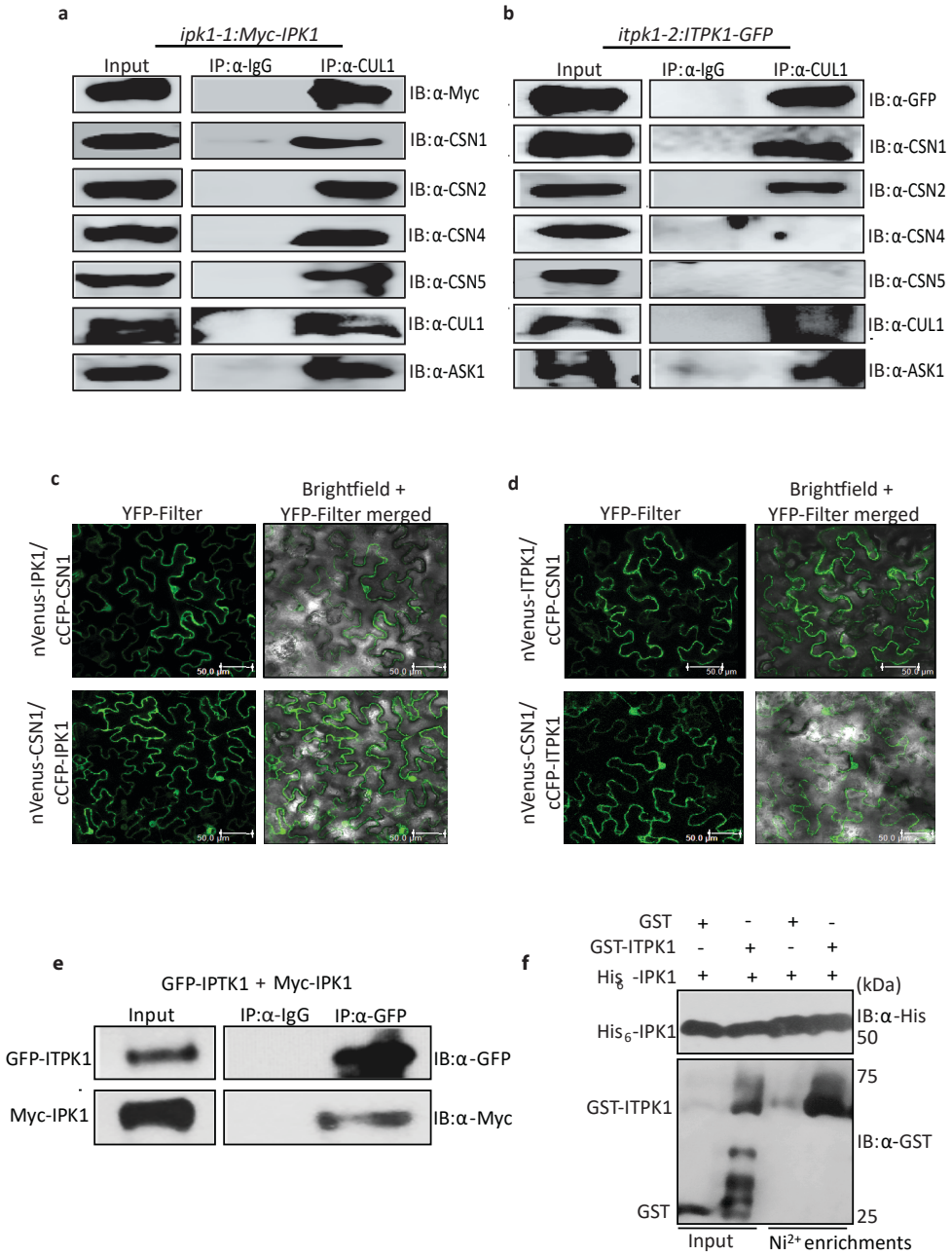

Fig. 1. IPK1 and ITPK1 interact with each other and with selective CSN or CRLs components *in planta*. a-b, Immuno-enrichments of IPK1 **(a)** or ITPK1 **(b)** from corresponding complemented lines (*ipk1-1: Myc-IPK1* or *itpk1-2:ITPK1-GFP*, respectively) and probed with anti-CSN1/2/4/5, anti-CUL1, or anti-ASK1 antibodies. IgG-agarose enrichments were used as negative controls. **c-d,** Bimolecular Fluorescence Complementation (BiFC) assays showing reciprocal combinations of **(c)** IPK1 and **(d)** ITPK1 interact with CSN1. Scale bar=50 µm. **e,** Co-immunoprecipitation of transiently expressed GFP-ITPK1 with Myc-IPK1. Immuno-enrichment was performed with anti-GFP antibody-conjugated agarose and probed with anti-GFP or anti-Myc antibodies. **f,** *In vitro* interactions of IPK1 with ITPK1. His_6-IPK1 was co-expressed with GST alone or GST-ITPK1 in *E. coli* cells. Ni^{2+}NTA-affinity enrichments were probed for His_6-IPK1 or GST-ITPK1 with anti-His or anti-GST antibodies, respectively. Migration positions of molecular weight markers (in kDa) and of His_6-IPK1, GST or GST-ITPK1 are shown on the right or left of each panel, respectively.

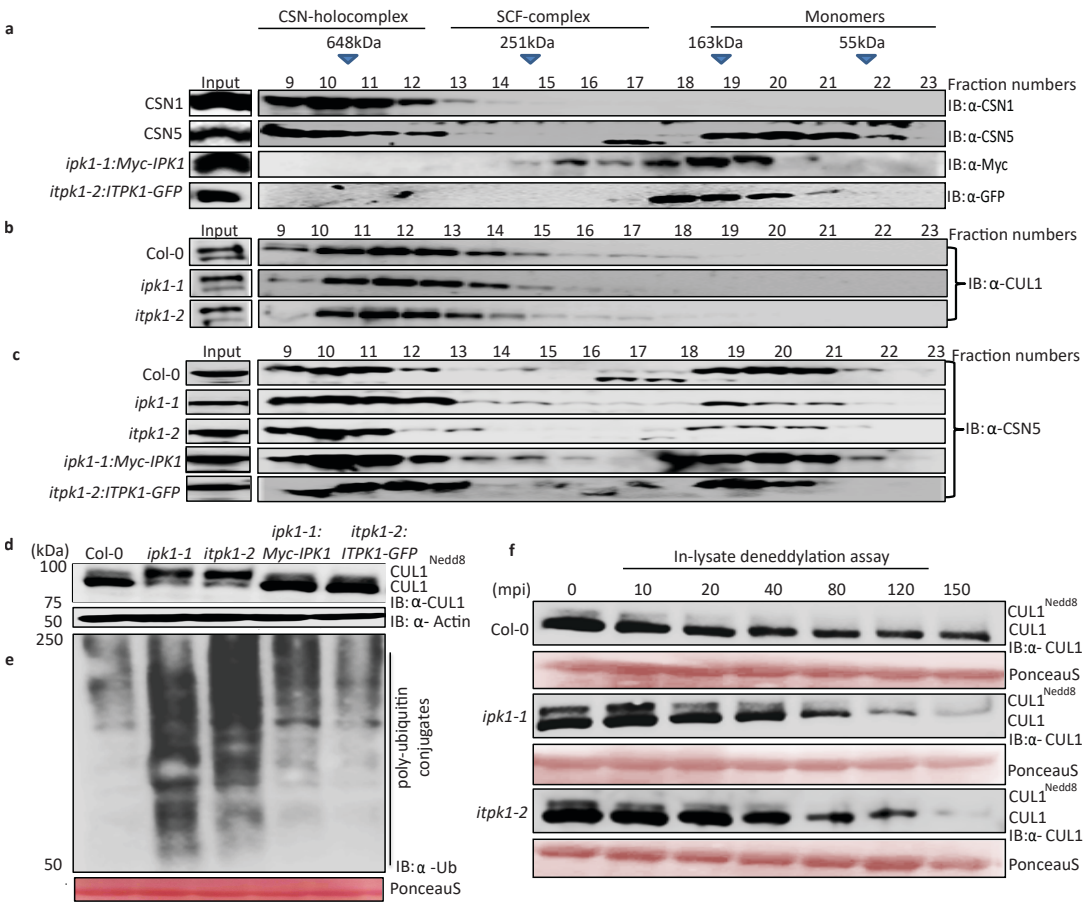

Fig. 2. CSN5 partitioning and deneddylase functions are affected in *ipk1-1* or *itpk1-2*. a, IPK1 or ITPK1 does not co-elute with the CSN holo-complex. **b,** CRL1 fractionation profiles are unchanged between Col-0, *ipk1-1* and *itpk1-2*. **c,** Enhanced CSN5 engagement on CSN holo-complex fractions in *ipk1-1* and *itpk1-2*. For fractionations, extracts were separated by size-exclusion chromatography and immuno-blotted with indicated antibodies. Right panels are immunoblots on input extracts. Fraction numbers are indicated above each lane. Numbers above arrowheads denote elution positions of molecular weight standards (in kDa). **d,** Increased neddylated CUL1 in *ipk1-1* or *itpk1-2*. **e,** Global polyubiquitin-conjugates are enhanced in *ipk1-1* or *itpk1-2*. For **d-e**, Total protein extracts were probed with anti-CUL1, anti-actin, or anti-Ubiquitin antibodies as indicated. **f,** CSN5-deneddylation deficiencies and lower CUL1 half-life in *ipk1-1* or *itpk1-2*. For in-lysate deneddylation assay total protein extracts incubated for indicated times (minutes post-incubation; mpi) were probed with anti-CUL1 antibodies. Migration position of molecular weight standards (in kDa) and neddylated ($CUL1^{Nedd8}$) or unneddylated (CUL1) cullin1 are shown. Anti-actin or Ponceau S staining demonstrate loadings controls.

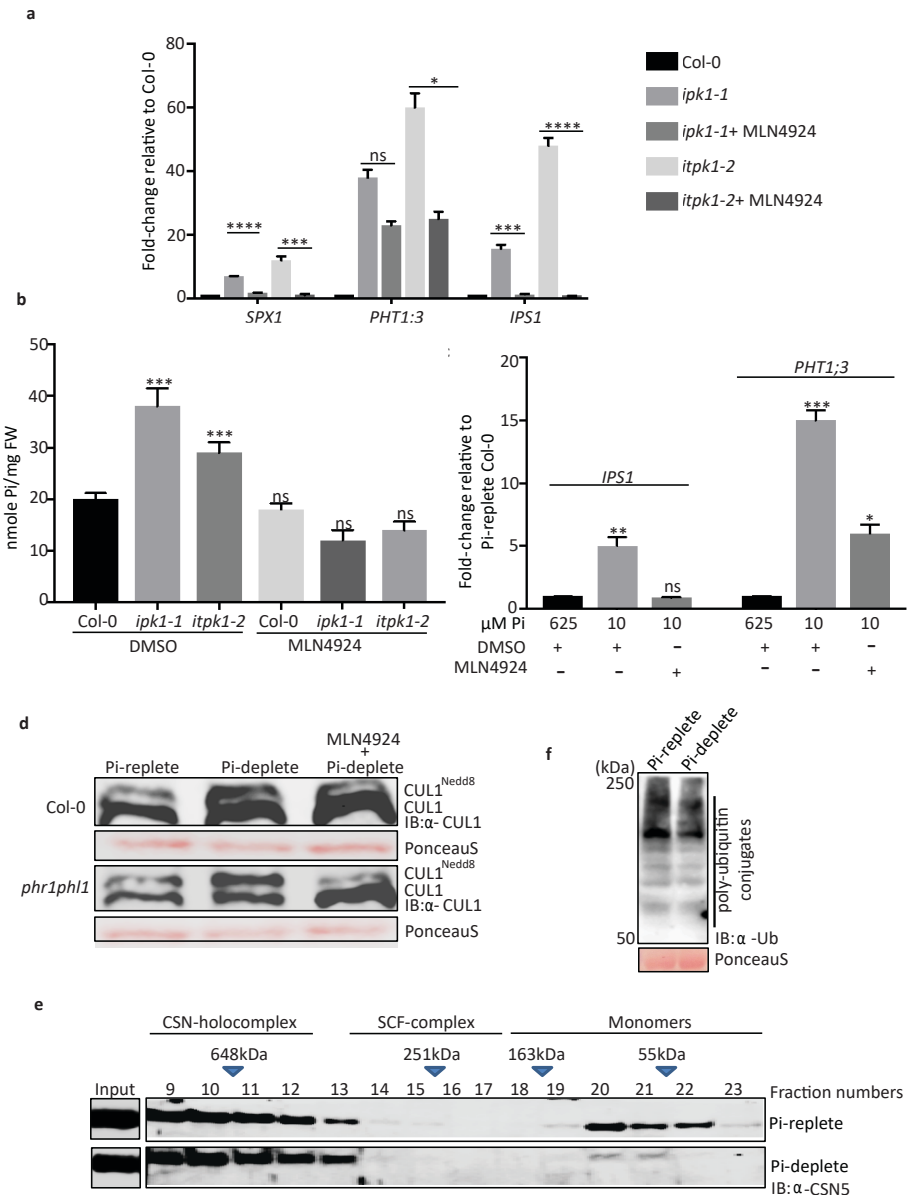

Fig. 3. CUL1 deneddylation rates are reduced during Pi-starvation. MLN4924 suppresses **a,** elevated PSI-gene expressions, and **b,** reduces endogenous Pi-levels in *ipk1-1* or *itpk1-2*. **c,** MLN4924 suppresses the induction of *PHT1;3* or *IPS1* expressions in Col-0 upon Pi-starvation. **d,** Enhanced CUL1-neddylation during Pi-deprivation is PHR1/PHL1-independent. **e,** Increased CSN5 partitioning on CSN holo-complex occur upon Pi-starvation. **f,** Global levels of polyubiquitin-conjugates are unperturbed during PSR. Gene expression changes were relative to *MON1* transcripts and reported as fold-change relative to Col-0 levels. Data is presented as mean ± SD (n=3 biological replicates of 3 plants in each). For Pi-estimation assays, data shown as mean ± SD (n= 6-7 plants). Asterisks denote significant differences from the reference sample. (Student's *t*-test; **P*<0.05, ***P* < 0.01; ****P* < 0.001, ****P*<0.0001. ns is not significant). For immunoblots, total protein extracts or fractions were probed with anti-CUL1 or anti-CSN5 or anti-ubiquitin antibodies, as indicated. Ponceau S staining show loadings controls. For Pi-deprivation/MLN4924 treatment assays, Seedlings grown in Pi-replete (625µM Pi) medium were either maintained or transferred to Pi-deplete (10 µM Pi) medium for three additional days in the presence of MLN4294 or absence (DMSO) during the shift, before being analyzed. Positions of molecular weight markers (in kDa) are shown.

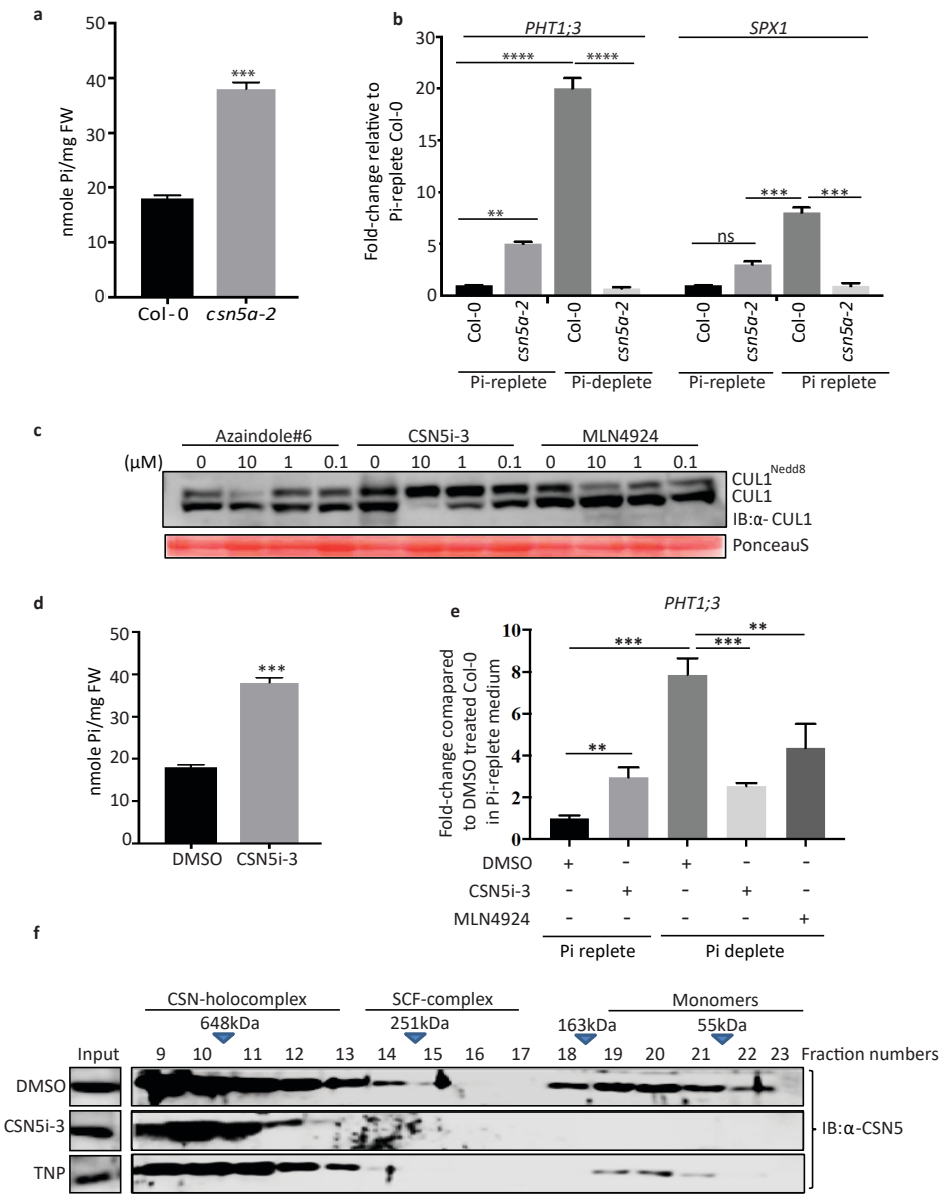

Fig. 4. The dynamics of CSN5 is essential for responding to phosphate-starvation. a, *csn5a-2* plants have elevated endogenous Pi levels. **b,** *csn5a-2* plants are deficient in inducing PSI-genes during Pi-starvation. **c,** CSN5i-3 shows dose-dependent inhibition in CUL1 deneddylation. Total protein extracts from Col-0, 24hrs post-treated with indicated doses of the inhibitors mentioned, were probed with anti-CUL1 antibodies. Ponceau S staining shows loading controls. **d,** CSN5i-3 treatment elevates endogenous Pi-levels. **e,** CSN5i-3 suppresses *PHT1;3* induction in Col-0 during phosphate-starvation. **f,** CSN5 is enriched in CSN holo-complex pools upon CSN5i-3 or TNP treatment. Fractionation was performed 24hrs post-inhibitor treatment and fractions immunoblotted with anti-CSN5 antibodies. For Pi-estimation assays, error bars show SD from mean (n=3 replicates of 5-6 plants each). For gene expression changes, *MON1* levels were used as internal controls and results reported as fold-change relative to untreated Pi-replete grown Col-0. Data is mean ± SD (n=3 replicates, 3-4 plants each). Statistical significance was calculated with Student's *t*-test and depicted with **P*<0.05, ***P* < 0.01; ****P* < 0.001, ****P*<0.0001. ns is not significant. For Pi-deprivation assays, plants grown in Pi-replete (625μM Pi) media were transferred for 3 days to Pi-deplete (10 μM Pi) media with or without indicated inhibitors before analysis.

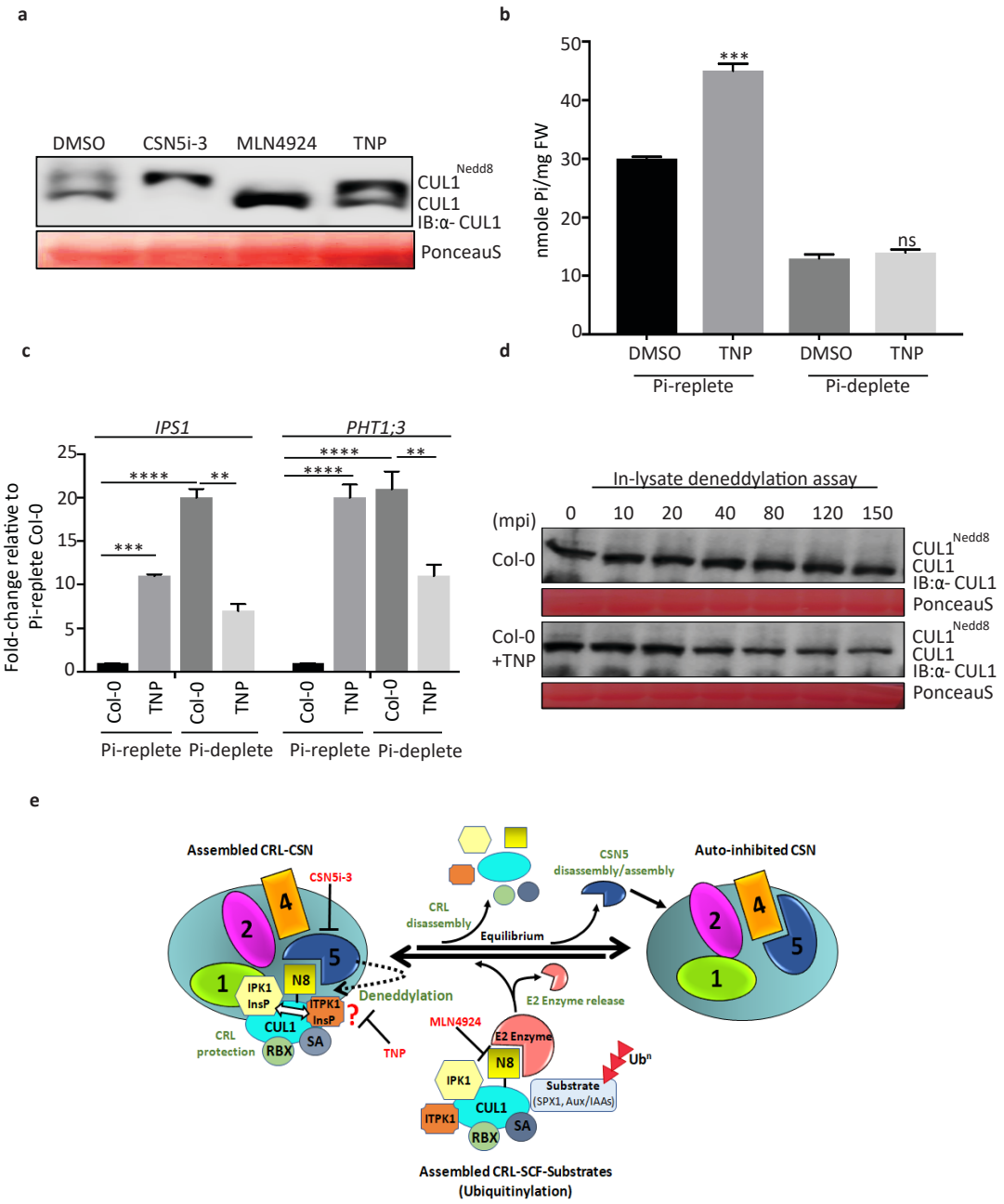

Fig. 5. ITPK1 activity regulates CSN5 dynamics and deneddylase functions. a, TNP treatment enhances pools of neddylated CUL1. Total protein extracts from Col-0 at 24hrs post-inhibitor treatment were immunoblotted with anti-CUL1 antibodies. **b,** TNP treatments increase endogenous Pi-content in Col-0. Error bars are mean ± SD (n=3 replicates of 5-6 plants each). **c,** TNP suppresses *IPS1* or *SPX1* in Col-0 upon Pi-starvation. For Pi-starvation, plants grown in Pi-replete medium were transferred for 3 days to Pi-deplete medium with or without TNP. Expression levels of *MON1* transcripts was used as internal reference. Error bars denote mean with SD (n=3 biological replicates of 3-4 plants each). Student's *t*-test was used to calculate statistical significance and shown as $^{**}P<0.01$, $^{***}P<0.001$, $^{****}P<0.0001$, ns not significant. **d,** TNP reduces CUL1 deneddylation and increases CUL1 instability. In-lysate deneddylation assay on Col-0 extracts post-24hrs TNP-treatment and then probed with anti-

759 CUL1 antibodies. Ponceau S staining indicates loadings control. **e,** Schematic representation
760 of IPK1-ITPK1 role on CRL-CSN association/dissociation equilibrium in plants. CSN holo-
761 complex platform offers protection to CRLs in absence of ubiquitinylation substrates (E2
762 enzyme prevented from binding due to mutual exclusion[43,44]) utilizing coordinated locale-
763 specific activities (bi-directional white arrows) of IPK1 and ITPK1. Stimulus/energy status-
764 dependent modulation in localized IPK1/ITPK1 activities (InsPs nature unknown; red question
765 mark) is coupled to CRL, CSN5 disassembly and CUL1 deneddylation. Auto-inhibited CSN
766 holo-complex is reconstituted by re-incorporating CSN5. Active CRL-SCF complex binds E2
767 ubiquitin enzyme to cause targeted ubiquitinylation (Ub^n) and degradation of substrates (such
768 as SPX1 or Aux/IAA repressors). Inhibitory functions of TNP, CSN5i-3 and MLN4924 are
769 indicated on the respective processes. CSN subunits are presented as numbers; CUL1, Cullin1;
770 RBX, RING H2 protein1; SA, substrate adapter, N8, Nedd8, IPK1, inactive IPK1, ITPK1,
771 inactive ITPK1, IPK1 InsP, active IPK1, ITPK1 InsP, active ITPK1.

772 **Extended Data Figure legends.**

773 **Extended Data Fig. 1. Complemented lines restore PSR defects of *ipk1-1* and *itpk1-2*. a,**
774 Endogenous Pi levels in Col-0, *ipk1-1*, *itpk1-2* and respective complemented lines *ipk1-1:Myc-*
775 *IPK1* or *itpk1-2:ITPK1-GFP*. Data is represented as mean with SD (n=3 replicates of 3-4 plants
776 each). **b,** Relative expression levels of *SPX1* in the indicated plants. Transcript levels were
777 normalized to internal standard *MON1* expressions and are reported as fold-change relative to
778 Col-0. Error bars indicate SD (n=3, three replicates of 3 plants each). Statistical significance
779 was calculated by Student's *t*-test and reported with asterisks **P*<0.05, ***P* < 0.01; ****P* <
780 0.001, ****P*<0.0001. ns is not significant.

781 **Extended Data Fig. 2. *In planta* interactions between IPK1, ITPK1 and CSN2.** BiFC assays
782 showing interactions of **a,** IPK1 with CSN2. **b,** ITPK1 with CSN2. **c,** IPK1 with ITPK1. **d,**
783 Lack of interactions between the negative control GUS with IPK1, ITPK1, CSN1 or CSN2 is
784 shown. Agrobacterium strains expressing the indicated BiFC vectors (mentioned on the left of
785 each panel) were co-infiltrated in *N. benthamiana* leaves. Infiltrated leaf areas were visualized
786 at 48 hpi (hours post-infiltration) under a confocal microscope and imaged with YFP and bright
787 field filters. Figures are representative of multiple images obtained for each BiFC
788 combinations. Scale bar=50μM.

789 **Extended Data Fig. 3. CSN4 fractionation profiles are not affected in *ipk1-1* or *itpk1-2*.**
790 Total protein extracts from indicated plants were separated by size-exclusion chromatography
791 and immuno-blotted with anti-CSN4 antibodies. Right panels show detection of CSN4 in input
792 extracts. Fraction numbers are marked. Numbers above the arrowheads denote the elution
793 positions of molecular weight standards (in kDa). Fractions corresponding to CSN holo-
794 complex, SCF-complex, and CSN4 monomers are indicated.

795 **Extended Data Fig. 4. CRL-CSN associations are not affected in *ipk1-1* or *itpk1-2*. a,**
796 Immuno-enrichment of CUL1 detects stoichiometrically similar amounts of CSN1 and CSN2
797 in *ipk1-1* or *itpk1-2* to Col-0. Total protein extracts were immunoprecipitated with either IgG
798 or anti-CUL1 antibodies and immunoblotted with anti-CUL1, anti-CSN1 or anti-CSN2
799 antibodies. Western blots on input extracts are shown on the left panels. Migration position of
800 molecular weight markers (in kDa) are indicated.

801 **Extended Data Fig. 5. Global levels of neddylated CUL1 are not enhanced in *vih2-4* or**
802 ***ipk2β-1* plants.** Total protein extracts from indicated plants was immunoblotted with anti-
803 CUL1 antibodies. Migration position of neddylated: unneddylated CUL1 ($CUL1^{Nedd8}$:CUL1)
804 are shown. Ponceau S stained membrane demonstrates equal loading controls.

805 **Extended Data Fig. 6. Pi-starvation does aggravate increased neddylated CUL1 in *ipk1-1***
806 **or *itpk1-2*.** Total protein extracts from indicated plants grown in Pi-replete (625μM Pi) medium
807 and then transferred for 3-days to Pi-deplete (10μM Pi) medium, were immunoblotted with
808 anti-CUL1 antibodies. Relative positions of $CUL1^{Nedd8}$:CUL1 are shown. Anti-actin
809 immunoblot shows comparable protein loadings.

810 **Extended Data Fig. 7. CUL1 deneddylation efficiencies but not stability is reduced upon**
811 **Pi-starvation.** In-lysate deneddylation assay was performed on total protein extracts from 14-
812 day-old Col-0 plants Pi-starved (10μM Pi) or Pi-sufficient (625μM Pi) for the last 3-days.
813 Extracts were incubated for the indicated times (minutes post-incubation, mpi) and immuno-
814 blotted with anti-CUL1 antibodies. Relative migration positions of $CUL1^{Nedd8}$:CUL1 are
815 shown. Ponceau S staining shows equal protein loadings.

816 **Extended Data Fig. 8. Pi-starvation does not alter CSN1 or CUL1 fractionation profiles**
817 **a,** CSN1 and CUL1 profiles under Pi-replete and Pi-deplete conditions. Size-exclusion
818 fractionation of total protein extracts from Col-0 grown for a total period of 14-days with the

819 last 3 days either in Pi-replete (625μM Pi) or Pi-deplete (10μM Pi) medium. Fractions were
820 immunoblotted with anti-CSN1 or anti-CUL1 antibodies. Fraction numbers and elution
821 positions of molecular weight standards are indicated. Fractions corresponding to CSN holo-
822 complex, SCF-complex and lower molecular weight pools are marked. **b,** Enhanced
823 accumulation of IPK1 and ITPK1 under Pi-deplete conditions. Total extracts prepared from
824 indicated plants with treatments as above and probed with anti-Myc or anti-GFP antibodies.
825 Ponceau S staining for Rubisco shows loadings controls.

826 **Extended Data Fig. 9.** The differential expression of PSI-genes in *csn* mutants with respect to
827 wild-type (Wt) are extracted from the microarray data reported in Dohmann et al (2008)[36]. The
828 heatmap is generated using Graphpad Prism 8.4.3 using double gradient Heatmap function.
829 The expression change is shown as $\log_2$FC(Fold-Change) values of different genes with Green
830 for downregulated genes, Red for upregulated genes and black for either genes which show no
831 change or the genes with expression values which are not significant (Adjusted $P > 0.10$).

832 **Extended Data Fig. 10. CSN5i-3 inhibits CUL1 deneddylation in Col-0 in dose-dependent**
833 **increments.** 14-day-old Col-0 plants were treated with indicated doses (in μM) of
834 Azaindole#6, CSN5i-3 or MLN4924 for 48hrs. Total proteins extracts were immunoblotted
835 with anti-CUL1 antibodies. Positions of neddylated ($CUL1^{Nedd8}$) and unneddylated CUL1 is
836 shown. Ponceau S staining shows comparable loading across samples.

837 **Extended Data Fig. 11.** CSN5 inhibitions suppresses induction of PSI-genes. **a,** CSN5i-3
838 suppresses *SPX1* induction in Col-0 during phosphate-starvation. **b,** Upregulated *IPS1*
839 expressions in *ipk1-1* or *itpk1-2* is suppressed in the presence of CSN5i-3. Gene expression
840 changes are relative to *MON1* levels. Data reported is mean ± SD (n=3 replicates, 3-4 plants
841 each). Statistical significance is according to Student's *t*-test and shown as $*P<0.05$, $**P< 0.01$;
842 $***P< 0.001$, $****P<0.0001$. ns is not significant. Pi-deprivation assays involved transfer of

843 Pi-replete (625μM Pi) grown plants to Pi-deplete (10μM Pi) medium with or without inhibitors
844 for 3 days before being analyzed.

845 **Extended Data Fig. 12. Supplemented $InsP_6$ does not affect CUL1 deneddylation rate or**
846 **stability. a,** In-lysate deneddylation assay on total protein extracts isolated from Col-0, *ipk1-*
847 *1*, or *itpk1-2* plants. Extracts were supplemented with or without 0.2μM $InsP_6$, incubated for
848 indicated times (minutes post-incubation; mpi) and probed with anti-CUL1 antibodies. **b,**
849 CUL1 neddylations remain comparable to Col-0 in *itpk4-1*. Total protein extracts were
850 immunoblotted with anti-CUL1 antibodies. Relative migrations of neddylated:unneddylated
851 CUL1 ($CUL1^{Nedd8}$:CUL1) are indicted. Loading controls are shown by Ponceau S staining.

852 **Supplementary Table 1.** List of oligonucleotide primers used in this study.

853

854

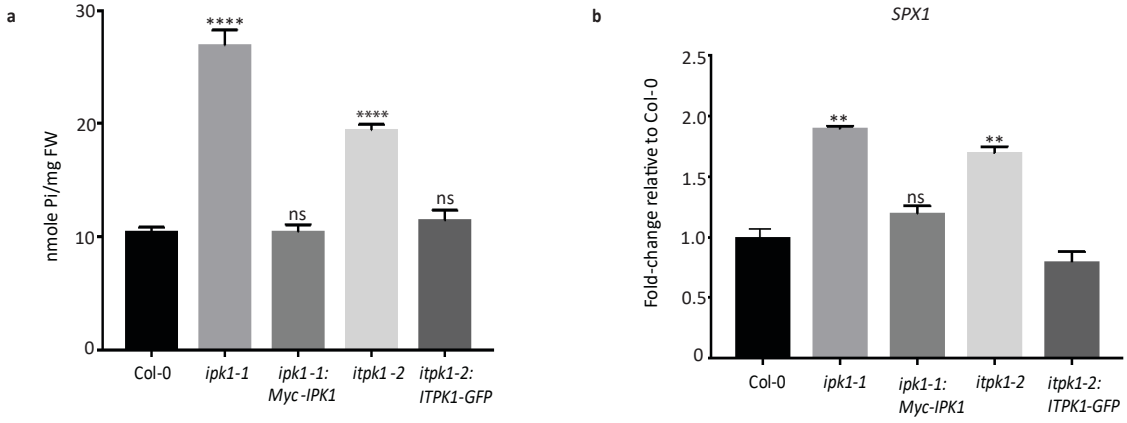

Extended Data Fig. 1. Complemented lines restore PSR defects of *ipk1-1* and *itpk1-2*. a, Endogenous Pi levels in Col-0, *ipk1-1*, *itpk1-2* and respective complemented lines *ipk1-1:Myc-IPK1* or *itpk1-2:ITPK1-GFP*. Data is represented as mean with SD (n=3 replicates of 3-4 plants each). **b,** Relative expression levels of *SPX1* in the indicated plants. Transcript levels were normalized to internal standard *MON1* expressions and are reported as fold-change relative to Col-0. Error bars indicate SD (n=3, three replicates of 3 plants each). Statistical significance was calculated by Student's *t*-test and reported with asterisks **P*<0.05, ***P* < 0.01; ****P* < 0.001, ****P*<0.0001. ns is not significant.

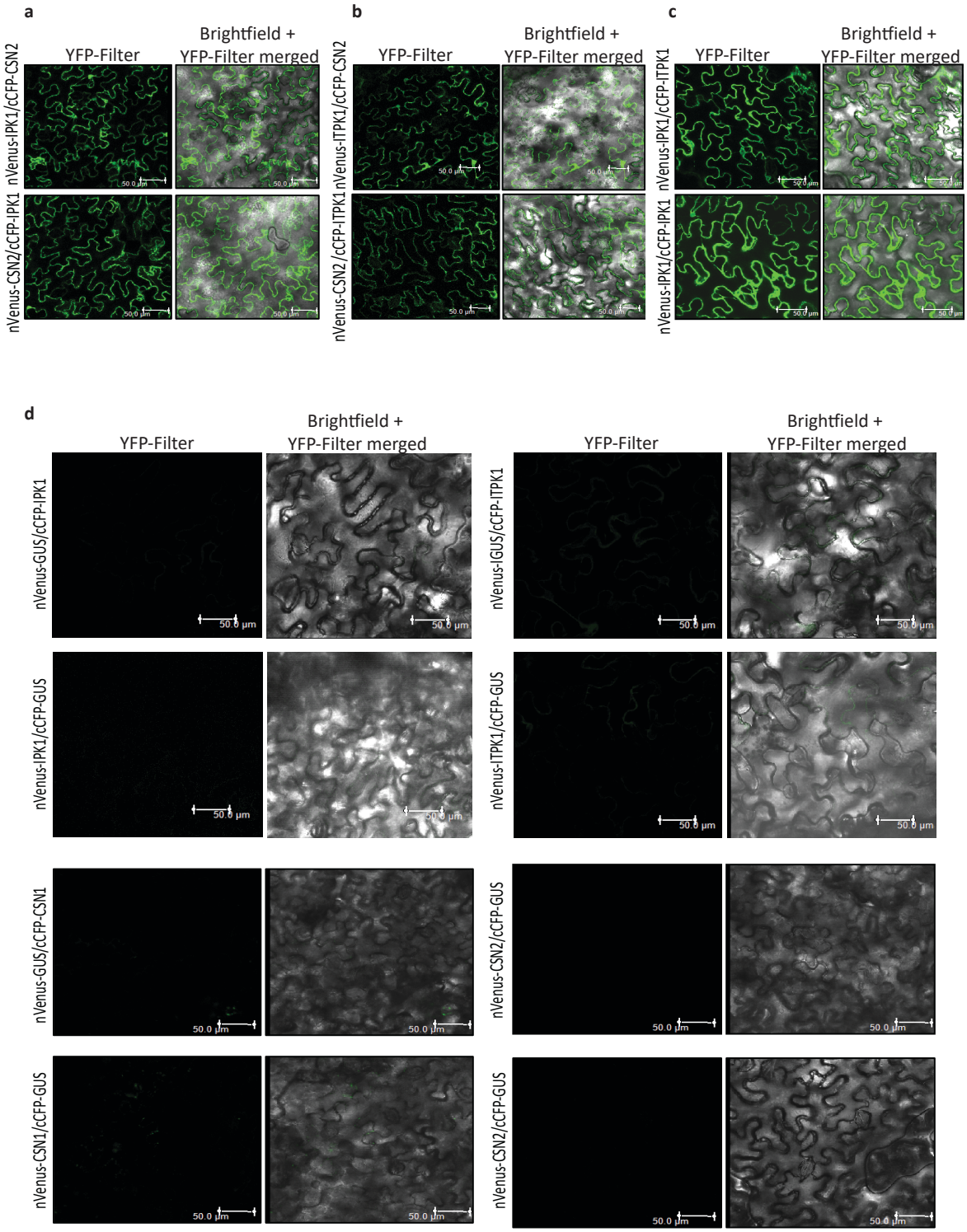

Extended Data Fig. 2. *In planta* interactions between IPK1, ITPK1 and CSN2. BiFC assays showing interactions of **a,** IPK1 with CSN2. **b,** ITPK1 with CSN2. **c,** IPK1 with ITPK1. **d,** Lack of interactions between the negative control GUS with IPK1, ITPK1, CSN1 or CSN2 is shown. Agrobacterium strains expressing the indicated BiFC vectors (mentioned on the left of each panel) were co-infiltrated in *N. benthamiana* leaves. Infiltrated leaf areas were visualized at 48 hpi (hours post-infiltration) under a confocal microscope and imaged with YFP and bright field filters. Figures are representative of multiple images obtained for each BiFC combinations. Scale bar =50µM.

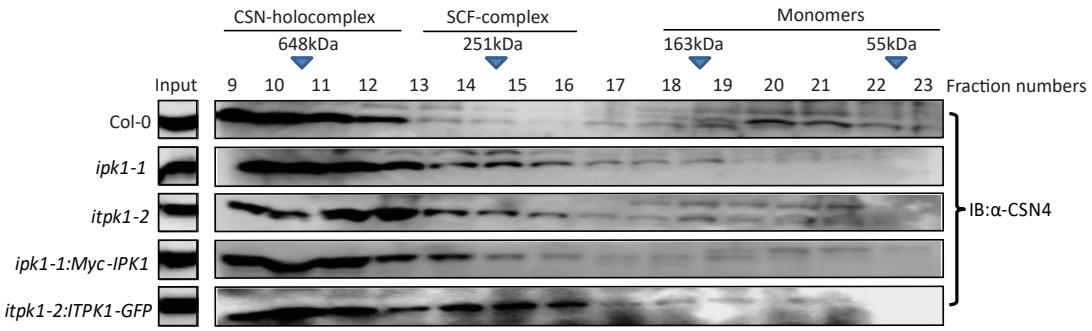

Extended Data Fig. 3. CSN4 fractionation profiles are not affected in *ipk1-1* or *itpk1-2*. Total protein extracts from indicated plants were separated by size-exclusion chromatography and immuno-blotted with anti-CSN4 antibodies. Right panels show detection of CSN4 in input extracts. Fraction numbers are marked. Numbers above the arrowheads denote the elution positions of molecular weight standards (in kDa). Fractions corresponding to CSN holo-complex, SCF-complex, and CSN4 monomers are indicated.

880

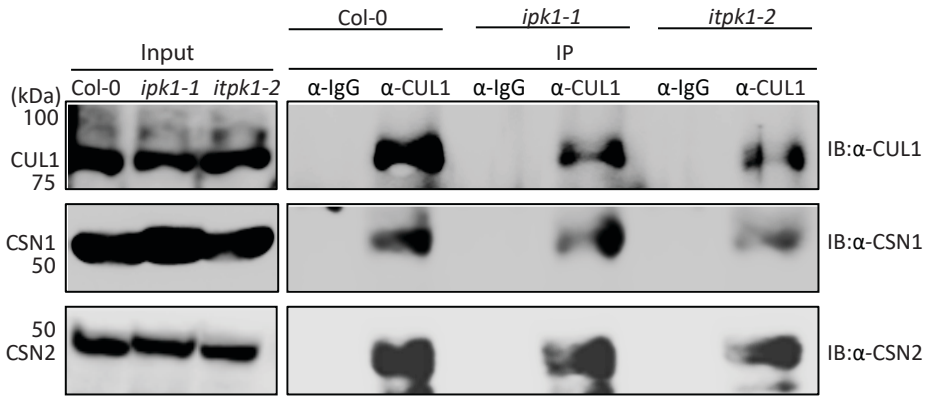

881

882 **Extended Data Fig. 4. CRL-CSN associations are not affected in *ipk1-1* or *itpk1-2*. a,**
883 Immuno-enrichment of CUL1 detects stoichiometrically similar amounts of CSN1 and CSN2
884 in *ipk1-1* or *itpk1-2* to Col-0. Total protein extracts were immunoprecipitated with either IgG
885 or anti-CUL1 antibodies and immunoblotted with anti-CUL1, anti-CSN1 or anti-CSN2
886 antibodies. Western blots on input extracts are shown on the left panels. Migration position of
887 molecular weight markers (in kDa) are indicated.

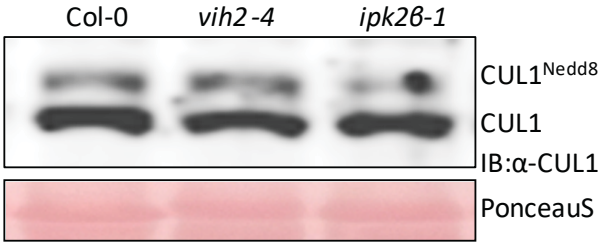

Extended Data Fig. 5. Global levels of neddylated CUL1 are not enhanced in *vih2-4* or *ipk2β-1* plants. Total protein extracts from indicated plants was immunoblotted with anti-CUL1 antibodies. Migration position of neddylated: unneddylated CUL1 ($CUL1^{Nedd8}$:CUL1) are shown. Ponceau S stained membrane demonstrates equal loading controls.

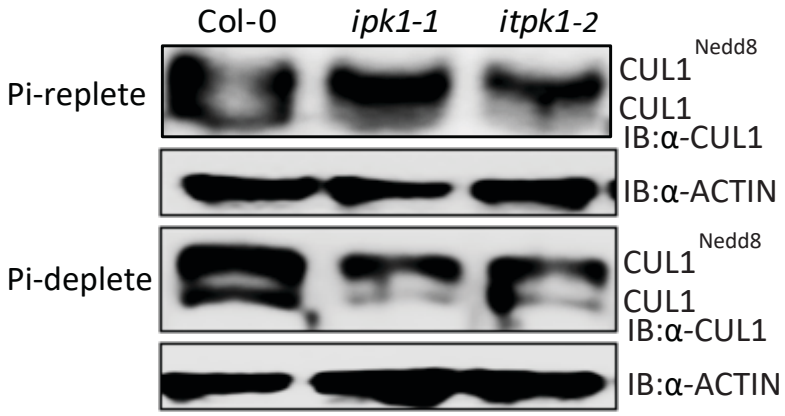

894

895 **Extended Data Fig. 6. Pi-starvation does aggravate increased neddylated CUL1 in *ipk1-1***
896 **or *itpk1-2*.** Total protein extracts from indicated plants grown in Pi-replete (625μM Pi) medium
897 and then transferred for 3-days to Pi-deplete (10μM Pi) medium, were immunoblotted with
898 anti-CUL1 antibodies. Relative positions of $CUL1^{Nedd8}$:CUL1 are shown. Anti-actin
899 immunoblot shows comparable protein loadings.

900

901

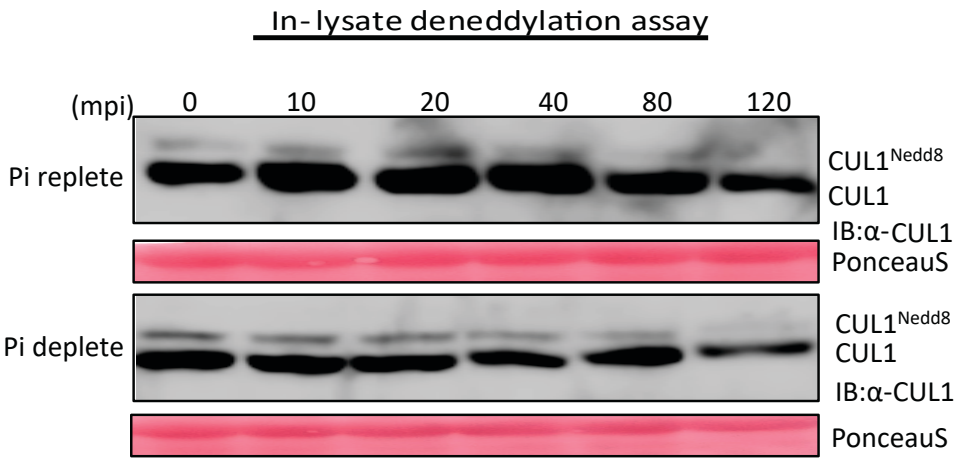

Extended Data Fig. 7. CUL1 deneddylation efficiencies but not stability is reduced upon Pi-starvation. In-lysate deneddylation assay was performed on total protein extracts from 14-day-old Col-0 plants Pi-starved (10μM Pi) or Pi-sufficient (625μM Pi) for the last 3-days. Extracts were incubated for the indicated times (minutes post-incubation, mpi) and immuno-blotted with anti-CUL1 antibodies. Relative migration positions of $CUL1^{Nedd8}$:CUL1 are shown. Ponceau S staining shows equal protein loadings.

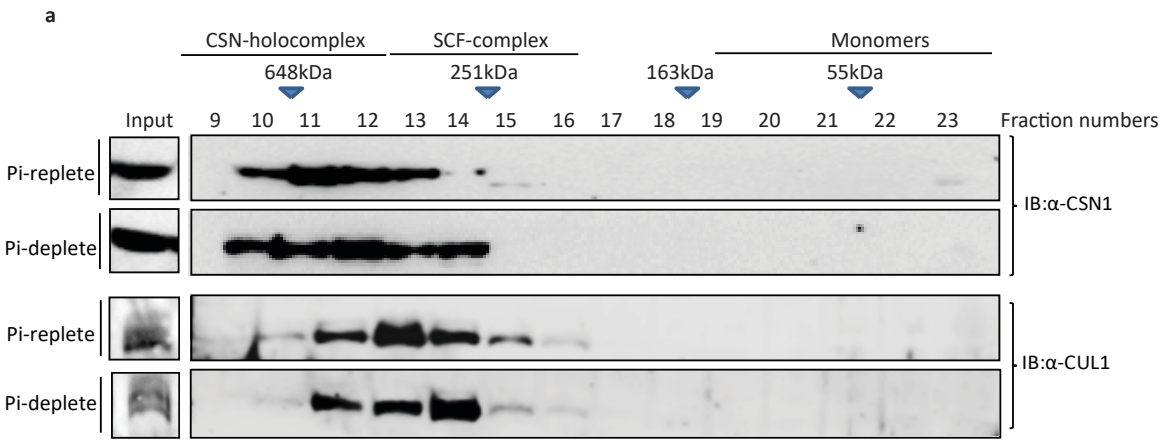

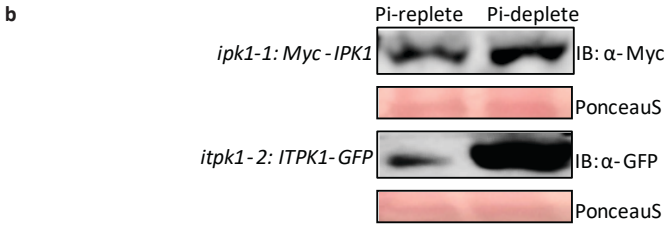

Extended Data Fig. 8. Pi-starvation does not alter CSN1 or CUL1 fractionation profiles a, CSN1 and CUL1 profiles under Pi-replete and Pi-deplete conditions. Size-exclusion fractionation of total protein extracts from Col-0 grown for a total period of 14-days with the last 3 days either in Pi-replete (625µM Pi) or Pi-deplete (10µM Pi) medium. Fractions were immunoblotted with anti-CSN1 or anti-CUL1 antibodies. Fraction numbers and elution positions of molecular weight standards are indicated. Fractions corresponding to CSN holo-complex, SCF-complex and lower molecular weight pools are marked. **b,** Enhanced accumulation of IPK1 and ITPK1 under Pi-deplete conditions. Total extracts prepared from indicated plants with treatments as above and probed with anti-Myc or anti-GFP antibodies. Ponceau S staining for Rubisco shows loadings controls.

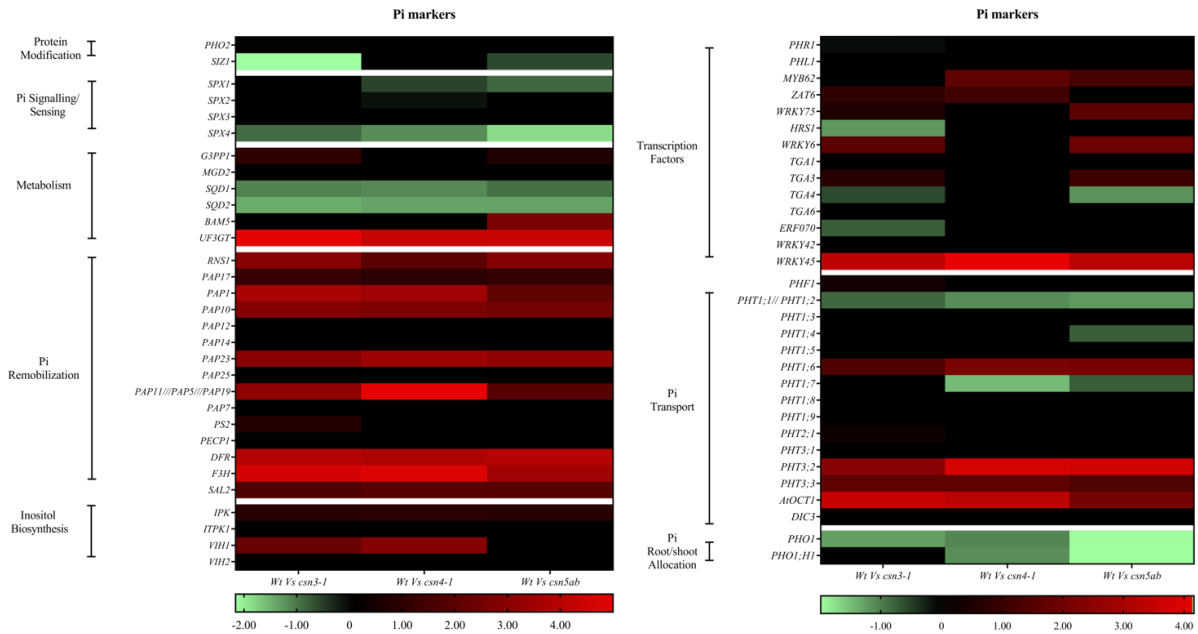

Extended Data Fig. 9. The differential expression of PSI-genes in *csn* mutants with respect to wild-type (Wt) are extracted from the microarray data reported in Dohmann et al (2008)[36]. The heatmap is generated using Graphpad Prism 8.4.3 using double gradient Heatmap function. The expression change is shown as $\log_2$FC(Fold-Change) values of different genes with Green for downregulated genes, Red for upregulated genes and black for either genes which show no change or the genes with expression values which are not significant (Adjusted $P > 0.10$).

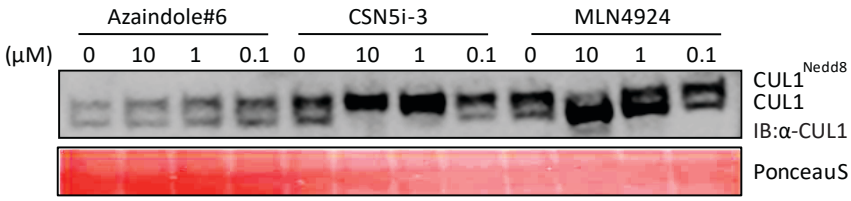

934

935 **Extended Data Fig. 10. CSN5i-3 inhibits CUL1 deneddylation in Col-0 in dose-dependent**
936 **increments.** 14-day-old Col-0 plants were treated with indicated doses (in μM) of
937 Azaindole#6, CSN5i-3 or MLN4924 for 48hrs. Total proteins extracts were immunoblotted
938 with anti-CUL1 antibodies. Positions of neddylated ($CUL1^{Nedd8}$) and unneddylated CUL1 is
939 shown. Ponceau S staining shows comparable loading across samples.

940

941

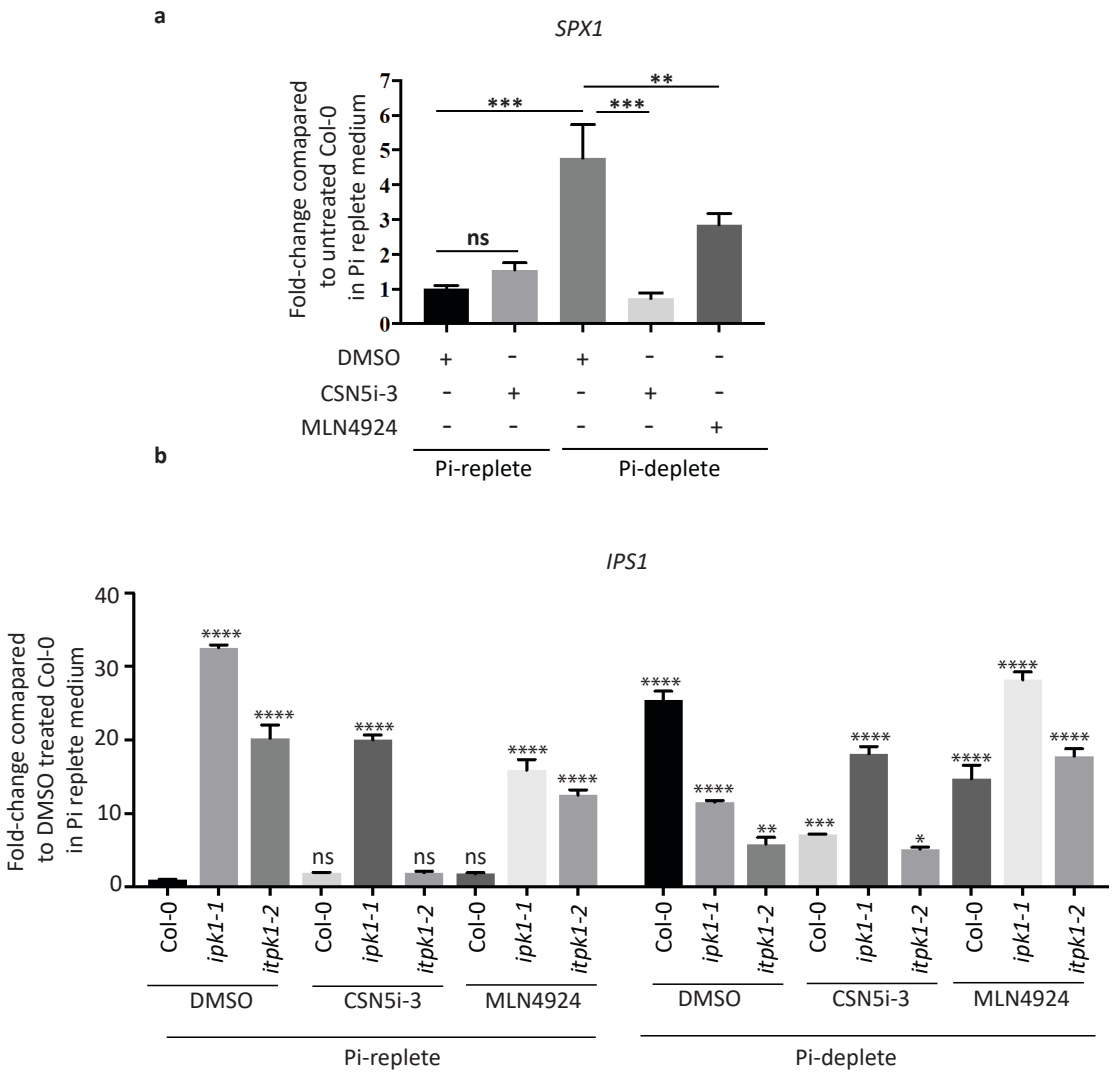

Extended Data Fig. 11. CSN5 inhibitions suppresses induction of PSI-genes. **a,** CSN5i-3 suppresses *SPX1* induction in Col-0 during phosphate-starvation. **b,** Upregulated *IPS1* expressions in *ipk1-1* or *itpk1-2* is suppressed in the presence of CSN5i-3. Gene expression changes are relative to *MON1* levels. Data reported is mean ± SD (n=3 replicates, 3-4 plants each). Statistical significance is according to Student's *t*-test and shown as **P*<0.05, ***P*< 0.01; ****P*< 0.001, *****P*<0.0001. ns is not significant. Pi-deprivation assays involved transfer of Pi-replete (625µM Pi) grown plants to Pi-deplete (10µM Pi) medium with or without inhibitors for 3 days before being analyzed.

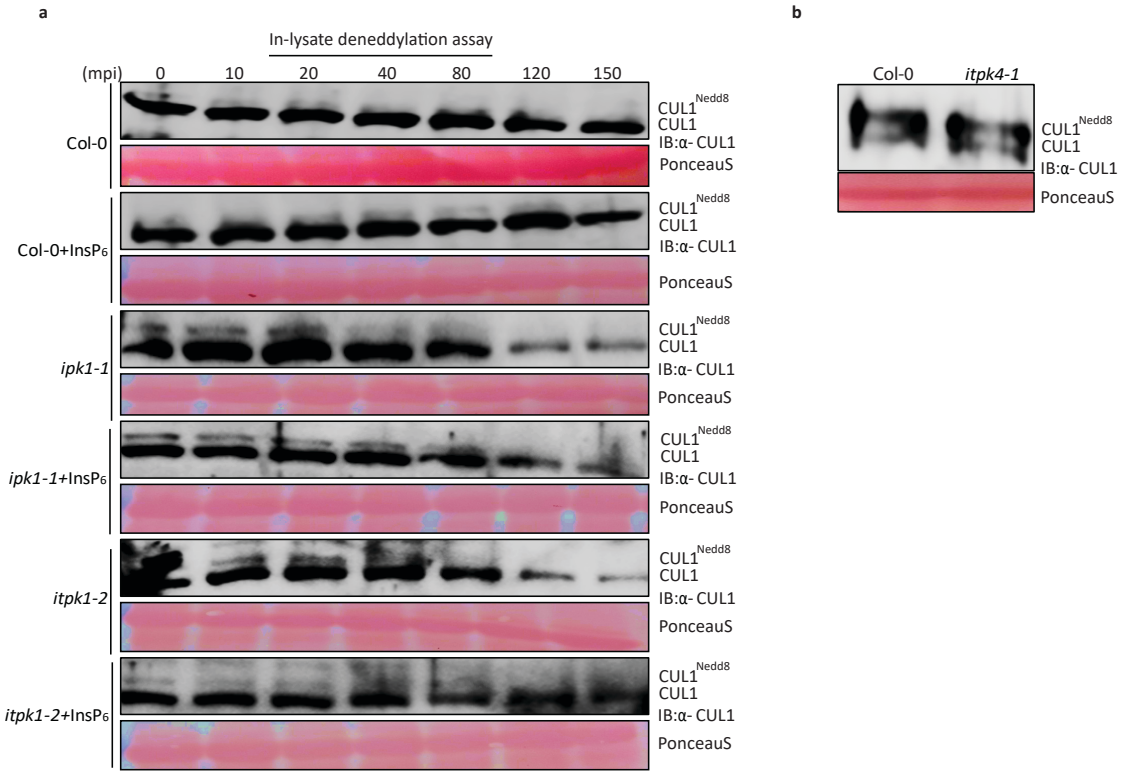

953

954 **Extended Data Fig. 12. Supplemented $InsP_6$ does not affect CUL1 deneddylation rate or**
955 **stability. a,** In-lysate deneddylation assay on total protein extracts isolated from Col-0, *ipk1-*
956 *1*, or *itpk1-2* plants. Extracts were supplemented with or without 0.2μM $InsP_6$, incubated for
957 indicated times (minutes post-incubation; mpi) and probed with anti-CUL1 antibodies. **b,**
958 CUL1 neddylations remain comparable to Col-0 in *itpk4-1*. Total protein extracts were
959 immunoblotted with anti-CUL1 antibodies. Relative migrations of neddylated:unneddylated
960 CUL1 ($CUL1^{Nedd8}$:CUL1) are indicted. Loading controls are shown by Ponceau S staining.

961

962

963 **Supplementary Table 1. Oligonucleotide primers used in this study.**

S. No	Primer Name	Primer Sequence (5' to 3')	Purpose
1.	attB1 *IPK1* For	GGGGACAAGTTTGTACAAAAAAGCAGGCTCAATGGAGATGATTTTGGAGG	Gateway cloning of IPK1 cDNA in pDONR207
2.	attB2 *IPK1* Rev	GGGGACCACTTTGTACAAGAAAGCTGGGTATTAGCTGTGGGAAGGTTTTGAG	Gateway cloning of IPK1 cDNA in pDONR207
3.	attB1 *ITPK1* For	GGGGACAAGTTTGTACAAAAAAGCAGGCTCAATGTCAGATTCAATCCAG	Gateway cloning of ITPK1 cDNA in pDONR207
4.	attB1 *ITPK1* Rev	GGGGACCACTTTGTACAAGAAAGCTGGGTATCAGACATGATTCTTCTTAGTG	Gateway cloning of ITPK1 cDNA in pDONR207
5.	attB1 *CSN1* For	GGGGACAAGTTTGTACAAAAAAGCAGGCTCA ATGGAGCGAGACGAAGAAGCGAGT	Gateway cloning of CSN1 cDNA in pDONR207
6.	attB2 *CSN1* Rev	GGGGACCACTTTGTACAAGAAAGCTGGGTATCAAAGTTTCCTTGCCGATCTGGCATG	Gateway cloning of CSN1 cDNA in pDONR207
7.	attB1 *CSN2* For	GGGGACAAGTTTGTACAAAAAAGCAGGCTCAATGGCTTCAGATGCTGACATGGAGGAC	Gateway cloning of CSN2 cDNA in pDONR207
8.	attB2 *CSN2* Rev	GGGGACCACTTTGTACAAGAAAGCTGGGTATTAACACAGTCGGCTGGTGATATTTGA	Gateway cloning of CSN2 cDNA in pDONR207
9.	qRT-PCR *PHT1;2* For	AGCCATCATTGGAGCCTTC	For qRT-PCRs
10.	qRT-PCR *PHT1;2* Rev	ACCTTAGCCTTGTCTTGATT	For qRT-PCRs
11.	qRT-PCR *IPS1* For	GCGTTTTAAGATATGGAGCAATG	For qRT-PCRs

12.	qRT-PCR *IPS1* Rev	CGAAGCTTGCCAAAGGATAG	For qRT-PCRs
13.	qRT-PCR *SPX1* For	GATTCCATTGTTGGAGCAAGA	For qRT-PCRs
14.	qRT-PCR *SPX1* Rev	AATCTTGTTAGCTTCTTCTATTGTA	For qRT-PCRs
15.	qRT-PCR *PHT1;3* For	AAACATTGTGAACCATGCTAACCCTT	For qRT-PCRs
16.	qRT-PCR *PHT1;3* Rev	GATAAACAAAATTGATTGGAATGACCACTA	For qRT-PCRs
17.	qRT-PCR MON1 For	AACTCTATGCAGCATTTGATCCACT	For qRT-PCRs
18.	qRT-PCR *MON1* Rev	TGATTGCATATCTTTATCGCCATC	For qRT-PCRs
19.	*ipk1-1* RP	TTTCAATCAAGGAATGCTTGG	Genotyping *ipk1-1*
20.	*ipk1-1* LP	ATGCTACGGGAAACCATTTTC	Genotyping *ipk1-1*
21.	*itpk1-2* RP	CCATGTCCCAGAAGAACTCAG	Genotyping *itpk1-2*
22.	*itpk1-2* LP	ACCAATATTCGATTCGATTCCACACG	Genotyping *itpk1-2*
23.	LB1.3	ATTTTGCCGATTTCGGAAC	T-DNA Left-border primer (for *ipk1-1*)
24.	LB3	TAGCATCTGAATTTCATAACCAATCTCGATACAC	T-DNA Left-border primer (for *itpk1-2*)
25.	AJHIFW2	GTTTTGGATTAGCATTAGTCCCCAAATC	Genotyping *csn5a-2* plants (Dohmann et al., 2005)
26.	AJH1RV2	TTCAAACATAAATGTGAAAAACAACAT	Genotyping *csn5a-2* plants (Dohmann et al., 2005)
27.	LBb1	CAGCGTGGACCGCTTGCTGCAACTCTCTCA	T-DNA Left-border primer (for *csn5a-2*)

			(Dohmann et al., 2005)
28.	*Bam*HI IPK1 For	CCGGATCCGAGATGATTTTGGAGGAG	Cloning IPK1 in *p*ET28a
29.	*Sal*I IPK1 Rev	GGGTCGACTTAGCTGTGGGAAGGTTTTG	Cloning IPK1 in *p*ET28a
30.	*Bam*HI ITPK1 For	GGGGATCCATGTCAGATTCAATCCA	Cloning ITPK1 in *p*GEX4T-3
31.	*Xho*I IPK1 Rev	GGCTCGAGTCAGACATGATTCTTCTT	Cloning ITPK1 in *p*GEX4T-3

964

965